MECHANISTIC DISSECTION OF INSIG-1, A MASTER REGULATOR OF CHOLESTEROL HOMEOSTASIS

APPROVED BY SUPERVISORY COMMITTEE

Michael S. Brown, M.D.

Joseph L. Goldstein, M.D.

Xiaodong Wang, Ph.D.

Richard G.W. Anderson, Ph.D.

John M, Abrams, Ph.D.

TO MY FAMILY

MECHANISTIC DISSECTION OF INSIG-1, A MASTER REGULATOR OF CHOLESTEROL HOMEOSTASIS

by

YI GONG

DISSERTATION

Presented to the Faculty of the Graduate School of Biomedical Sciences

The University of Texas Southwestern Medical Center at Dallas

In Partial Fulfillment of the Requirements

For the Degree of

DOCTOR OF PHILOSOPHY

The University of Texas Southwestern Medical Center at Dallas

Dallas, Texas

January, 2006

ACKNOWLEDGEMENTS

I am deeply grateful to my mentors, Dr. Michael S. Brown and Dr. Joseph L. Goldstein, for their guidance and support during my graduate training. They provide me the models of how to do rigorous science, as well as a rich scientific environment to learn and to grow up.

I also like to thank the members of my dissertation committee, Xiaodong Wang, Dick Anderson, and John Abrams, for spending their time and effects in completing this body of work.

Furthermore, I would like to express my appreciation to the team members who are currently working on Insig degradation. Jin Ye and Joon No Lee gave me enormous help on this project. The addictive or synergistic effects from our collaboration made the whole journey fruitful and joyful.

I am really fortunate to work in a friendly environment with so many respectable colleagues. I must thank Peter Espenshade who guided me through the first several months. Russell DeBose-Boyd always has great advice whenever I asked for. Rob Rawson kindly shared his experience in somatic cell genetics. Peter Lee generously provided reagents for the critical experiments. Arun Radhakrishnan taught me valuable lesions on lipid and detergent. Yuri Bashmakov provided me the crucial Insig antibody.

My deepest thanks to Lisa Beatty, Angela Carroll, Marissa Hodgin, Lorena Avila, Debora Morgan, Tammy Dinh, and Jeff Cormier for their excellent technical assistance; to Lu Li, Jiafu Ou, Guosheng Liang, Liping Sun, and Ronak Lakhia for their warm and insightful

discussion; to Kay Pokladnik, Jeri Rogers, Mary Hestand, and Nancy Heard for their generous help and advice.

This work is dedicated to my family. I want to thank my parents for giving their every best to their daughter and let her choose her own path. I also want to thank my husband Ge for giving his big heart and making me a stronger and better person everyday.

MECHANISTIC DISSECTION OF INSIG-1, A MASTER REGULATOR OF CHOLESTEROL HOMEOSTASIS

Publication No._____

Yi Gong, Ph.D.

The University of Texas Southwestern Medical Center at Dallas, 2006

Supervising Professors: Michael S. Brown, M.D. and Joseph L. Goldstein, M.D.

Insigs are polytopic membrane proteins of the endoplasmic reticulum (ER) that regulate lipid synthesis by controlling the sterol-mediated vesicular transportation of sterol regulatory element binding proteins (SREBPs). SREBPs are ER bound transcription factors that form complexes with Scap. In sterol-depleted cells, Scap escorts SREBPs from the ER to the Golgi apparatus, where SREBPs are proteolytically cleaved to liberate the nuclear fragments that activate genes for cholesterol synthesis and uptake. When sterols overaccumulate in cells, the Scap/SREBP complex is retained in the ER by the anchor proteins called Insigs.

In this thesis I describe the formation of a complex between Insig-1 and Scap in a sterol regulated fashion which facilitates the ER retention of Scap. To understand the molecular basis of the interactions between Insig-1 and Scap, I use a site-directed mutagenesis approach to select residues in Insig-1 that are essential for Insig-1/Scap complex formation. This study reveals a functional role for the amino acid Asp-205, which is located at the beginning of the fourth loop of Insig-1. Mutation of this aspartic acid to alanine produces an inactive Insig-1 that no longer binds to Scap, and leads to sterol-resistant processing of SREBPs.

Mammalian cells express two Insig proteins differ in their mode of control. Insig-1, but not Insig-2, is an SREBP target gene. Also, Insig-1 protein is degraded more rapidly than Insig-2. Thus, Insig-1 is the focus of the study. I further demonstrate that degradation of Insig-1 is regulated by sterols. When ER cholesterol content is low, Insig-1 is ubiquitinated on lysines 156 and 158 and degraded in proteasomes. Sterol-induced binding of Insig-1 to Scap prevents Insig-1 ubiquitination and degradation. The dynamic change in Insig-1 protein stability, together with its transcriptional control by nuclear SREBPs, creates a new model for the convergent inhibition of SREBP processing and cholesterol supply in animal cells. Taken together, these studies established Insig-1 as the master regulator in the cholesterol homeostasis.

TABLE OF CONTENTS

PRIOR PUBLICATIONS

Gong, Y., Lee, J.N., Lee, P.C.W., Goldstein, J.L., Brown, M.S. and Ye, J. (2006). Sterol-regulated ubiquitination and degradation of Insig-1 creates a convergent mechanism for feedback control of cholesterol synthesis and uptake. Cell Metab 3, 15-24.

Lee, J.N., Gong, Y., Zhang, X., and Ye, J. (2006). Proteasomal degradation of ubiquitinated Insig-1 is determined by serine residues flanking ubiquitinated lysines. Manuscript submitted.

Yang, T., Espenshade, P.J., Wright, M.E., Yabe, D., Gong, Y., Aebersold, R., Goldstein, J.L., and Brown, M.S. (2002). Crucial step in cholesterol homeostasis: sterols promote binding of SCAP to INSIG-1, a membrane protein that facilitates of SREBPs in ER. Cell 110, 489-500.

LIST OF FIGURES

LIST OF ABBREVIATIONS

25-HC	25 hydroxycholesterol
ALLN	N-acetyl-leucinal-leucinal-norleucinal
bHLH-Zip	basic helix-loop-helix leucine zipper
BN-PAGE	blue native polyacrylamide gel electrophoresis
CHO	Chinese hamster ovary
CHX	cycloheximide
CMV	cytomegalovirus
COP	coat protein
ER	endoplasmic reticulum
FCS	fetal calf serum
HPCD	hydroxypropyl-β-cyclodextrin
HMG CoA	3-hydroxy-3-methylglutaryl coenzyme A
LDL	low-density lipoprotein
LPDS	lipoprotein-deficient serum
NPC 1	Niemann-Pick C1
ORF	open reading frame
PAGE	polyacrylamide gel electrophoresis
PBS	phosphate buffered saline
S1P	site 1 protease
S2P	site 2 protease
Scap	SREBP cleavage-activating protein

SDS	sodium dodecyl sulfate
SRD	sterol regulatory defective
SREBP	sterol regulatory element binding protein
SSD	sterol sensing domain
TK	thymidine kinase
TM	transmembrane
Ub	ubiquitin

CHAPTER 1 GENERAL INTRODUCTION

Feedback regulation of cholesterol metabolism

Cholesterol is essentially required for cell growth and maintenance. Because of its hydrophobic character, free cholesterol is located in the membrane of the cells, where it modulates the fluidity, and creates membrane rafts that facilitate the activities of signaling molecules (Anderson et al., 1998; 2002; Simons and Ikonen, 1997; 2000). In addition to its general function in membrane structure and dynamics, cholesterol is also a precursor of all steroid hormones and bile acids, and it plays a crucial role in the formation of the myelin sheath that surrounds axons. In early development, cholesterol is covalently attached to Hedgehog, a morphogen essential for embryonic patterning (Mann and Beachy, 2004). However, the deleterious effect of cholesterol is also well stated in the pathogenesis of human disease. Excess cholesterol in the blood can lead to cholesterol gallstones, xanthomas, and most importantly atherosclerotic vascular diseases, which are leading causes of death in Western countries. Therefore, cholesterol metabolism must be tightly regulated.

The cholesterol biosynthetic pathway is well known to undergo end-product feedback suppression, as is the cholesterol uptake from plasma low-density lipoprotein (LDL) from earlier studies in familial hypercholesterolemia (Anderson et al., 1976; 1977; Brown and Goldstein, 1986). Thus, homeostasis is achieved mainly by balancing *de novo* synthesis and uptake from the cholesterol rich LDL particles. When cellular sterol falls, the level of LDL receptor rises, and exogenous cholesterol is taken from LDL, which enters the cell by receptor-mediated endocytosis. Endogenous synthesis of cholesterol is

also elevated through the high activities of enzymes involved in cholesterol biosynthetic pathway including the rate-limiting enzyme, 3-hydroxy-3-methylglutaryl coenzyme A (HMG CoA) reductase. The resulting increase in the cholesterol levels from both sources relieves the cellular cholesterol demands. Once sterol content exceeds the needs of the cells, the level of LDL receptor declines and the activities of HMG CoA reductase and other enzymes are dramatically inhibited as a result of negative feedback repression. Through these regulatory mechanisms, cells keep their level of cholesterol remarkably constant despite wide fluctuations in cholesterol requirements and exogenous supply.

Sterol-mediated transcriptional regulation

The molecular basis of the feedback regulation of cholesterol synthesis and uptake relates to the discovery of the sterol-mediated regulation of transcription. The cloning of the genes for LDL receptor, HMG CoA reductase, and HMG CoA synthase has revealed that their mRNA levels are coordinately regulated by sterols. Transcription of these sterol-sensitive genes is enhanced under conditions of cholesterol deprivation, and diminished when cells are overloaded with sterols (Brown and Goldstein, 1990). Mutation studies in the 5' flanking regions of these genes traced the principle regulatory activity to a short segment that contained a closely related sequence, which has been designated sterol regulatory element-1 (SRE-1) (Südhof et al., 1987).

The sterol regulatory element binding proteins (SREBPs) were purified from nuclear extracts of cultured human HeLa cells by virtue of their ability to bind SRE sequences (Wang et al., 1993). Later cDNA cloning revealed that mammalian cells express three closely related isoforms of SREBP, known as SREBP-1a, SREBP-1c, and

SREBP-2. SREBP-1a and –1c are produced from the same gene through the use of different promoters and alternative splicing. All three SREBPs belong to the basic helix-loop-helix leucine zipper (bHLH-Zip) family of transcription factors (Yokoyama et al, 1993; Hua et al, 1993). However, unlike other bHLH-Zip members, SREBPs are intrinsic membrane proteins of the endoplasmic reticulum (ER), and share a similar tripartite structure consisting of: (1) an NH_2-terminal transcription factor domain of ~480 amino acids; (2) a membrane anchoring domain of ~80 amino acids that comprises two transmembrane segments; and (3) a COOH-terminal regulatory domain of ~590 amino acids. Both the NH_2- and COOH- termini of SREBPs project into the cytosol and the central hydrophilic loop faces the lumen of the ER (Brown and Goldstein 1997; 1999).

In order to activate the transcription of the target genes, SREBPs have to be transported from ER to nucleus where they bind to the SREs. It is now clear that the release of active nuclear SREBPs (nSREBPs) from the membrane is achieved by sterol regulated ER-to-Golgi transport followed by two sequential proteolytic events. The process is initiated when the newly synthesized SREBPs bind to SREBP cleavage-activating protein (Scap) via their COOH-terminal regulatory domains (Sakai et al., 1997). SCAP is a polytopic ER protein of 1276 amino acids, which can be divided broadly into two domains (Nohturfft et al., 1998). The hydrophilic COOH- terminal 546 amino acids project into the cytosol where it binds to the cytosolic domain of SREBPs. The hydrophobic NH_2-terminal 730 amino acids consist of eight membrane-spanning helices, of which helices 2-6 constitute the sterol-sensing domain (Hua et al., 1996; Nohturfft et al., 1998). Scap functions as a sensor of the sterols and an escort protein for SREBPs. In sterol-depleted cells, the Scap/SREBP complex exits the ER in COPII-coated

vesicles and transports to the Golgi apparatus where SREBPs are cleaved by two proteases (S1P and S2P, respectively) in a process termed regulated intramembrane proteolysis (RIP) (Brown et al., 2000). Once the site-2 cleavage has occurred, the soluble NH_2-terminal transcriptional domains of SREBPs are now free to translocate to the nucleus where they activate transcription of target genes for cholesterol supply. When cholesterol builds up in ER membranes, the Scap/SREBP complex fails to exit the ER, proteolytic processing of SREBPs is abolished, and transcription of target genes declines (Nohturfft et al., 2000; Espenshade et al., 2002; Sun et al., 2005;).

Insigs in cholesterol homeostasis

Then, how do sterols control the ER-to-Golgi exit of the Scap/SREBP complex? Both genetic and biochemical evidence indicate that sterol-mediated retention of the Scap/SREBP complex by Insig, another polytopic membrane protein, is the key regulatory step in the cholesterol homeostasis. Back in 1996 when Scap was first cloned in CHO cells, it was found that overexpression of Scap led to constitutive Scap/SREBP transport that could no longer be suppressed by sterols (Hua et al., 1996). Similar results were observed when truncated Scap containing the sterol-sensing domain (TM1-6) was overexpressed (Yang et al., 2000). As a control, overexpression of a shorter segment of Scap (TM1-5) which has an incomplete sterol-sensing domain failed to release the Scap/SREBP complex. These results strongly suggest the existence of a saturable protein that binds to the sterol-sensing domain of Scap and holds the Scap/SREBP complex in the ER. Through affinity purification and tandem mass spectrometry analysis, Insig-1 was subsequently identified as the retention protein that coprecipitated only with Scap

(TM1-6), but not Scap (TM1-5). In the same year, Insig-2 was identified on the basis of its high sequence identity.

Soon after Insigs were identified as the retention factors for Scap/SREBP complex, a second action of Insigs was discovered in the feedback regulation of cholesterol synthesis. Namely, Insigs mediate the rapid proteolytic degradation of HMG CoA reductase (Sever et al., 2003a; 2003b). Like Scap, HMG CoA reductase is synthesized on ER membranes. The catalytic domain of the enzyme is attached to the membrane by virtue of an NH_2-terminal segment that contains eight membrane-spanning helices. Like Scap, the membrane-embedded portion of HMG CoA reductase contains a sterol-sensing domain. When sterols accumulate in ER membranes, they trigger the binding of HMG CoA reductase to Insigs, initiating a process by which HMG CoA reductase is ubiquitinated and degraded. When cells are depleted of sterols, HMG CoA reductase has an extended lifetime and the amount of active enzyme increase, this contributes to an increase in cholesterol synthesis in sterol-depleted cells.

The two known human Insig isoforms, Insig-1 and -2, are 59% identical over their lengths of 277 and 225 amino acids, respectively. Both are deeply embedded in ER membranes through the presence of six membrane-spanning helices (Feramisco et al., 2004). The main structure differences are confined to the hydrophilic NH_2- and COOH-terminal regions. Insig-2 lacks the NH_2-terminal 50 amino acids of Insig-1. In cultured cells, Insig-1 and Insig-2 are functionally similar in that overexpression of either one can cause the ER retention of the Scap/SREBP complex, and activate sterol-dependent degradation of HMG CoA reductase (Yabe et al., 2002; Sever et al., 2003). Combined knockdown of both Insig levels by RNA interference leads to an increase in nuclear

SREBPs (nSREBPs) that are not suppressed by sterols, and a marked raise in HMG CoA reductase levels owing to a failure of feedback degradation (Adams et al., 2003). *In vivo* studies in Transgenic Insig-1 mice showed that basal levels of all nuclear SREBPs (nSREBPs) are reduced. Plasma cholesterol and triglycerides levels are significantly declined. In addition to that, overexpression of this retention molecule renders the liver much more sensitive to sterol-mediated feedback suppression of lipid synthesis (Engelking et al., 2004). Conversely, the double knockout mice of Insig-1 and -2 overaccumulated cholesterol and triglycerides in liver, and the lipid synthesis and feedback response are severely blunted (Engelking et al., 2005).

Despite the functional similarities between Insig-1 and Insig-2, they are differentially regulated at multiple levels. Insig-1 is itself a target of nSREBPs, its mRNA level rises and falls coordinately with nSREBP (Luong et al., 2000; Horton et al., 2002). The Insig-2 gene has two promoters/enhancers that give rise to two transcripts with different noncoding first exons, but identical coding exons. In cultured cells one of these transcripts, designated Insig-2b, is unvarying and is not influenced by nSREBP levels. The other transcript, Insig-2a, is expressed nearly exclusively in the liver, and is negatively regulated by insulin (Yabe et al., 2002). Recently, another layer of posttranscriptional control was discovered that Insig-1 and -2 have different protein turnover rate. Insig-1 is rapidly degraded when general protein synthesis is blocked in cells under hypotonic stress, while Insig-2 is not affected because of its slower turnover rate (Lee and Ye, 2004).

Sterol-sensing of SREBP pathway

In general the function of sterol sensing refers to all cellular adaptive changes in response to cholesterol flux, specifically it refers to the feedback regulation by SREBPs. The importance of this function was originally observed in mutant cell lines with defects in Scap protein (Rawson et al., 1999). In mutant cells lacking Scap, SREBPs are not processed proteolytically, and the cells require exogenous cholesterol for growth. The opposite phenotype, sterol resistance, occurs in cells with one of three point mutations within the sterol-sensing domain of Scap, D433N, Y298C, or L315F. All three mutations abolish sterol-induced binding to Insigs and thereby render Scap insensitive to sterols. As a result, mutant Scap constitutively escorts SREBP to the Golgi even when cellular sterol levels are high, a condition eventually leads to massive cholesterol overproduction (Hua et al., 1996; Nohturfft et al., 1998; Yabe et al., 2002).

In addition to Scap mutants, there are two other classes of sterol regulatory defective (SRD) cells that fail to properly sense sterol-mediated transcription repression. Class I mutants produce a truncated form of SREBP-2 protein that never attaches to membranes, so it enters the nucleus regardless of sterol content (Yang et al., 1994; 1995). Class II mutants include SRD-14 and SRD-15 cells (Sever et al., 2004; Lee et al., 2005). Both are Insig deficient cell lines. SRD-14 cells are genetically defected in Insig-1 due to a partial deletion of the *Insig-1* gene, therefore, the mutant cells have no Insig-1 mRNA and protein, but keep the normal amount of Insig-2. As a result of their Insig-1 deficiency, the SRD-14 cells have a partial resistance to sterol-mediated SREBP processing. 5hr exposure of sterols has no effect on SREBP cleavage, however, longer

treatment of sterols does block SREBP processing, presumably caused by the remaining Insig-2 proteins. SRD-15 cells are further selected on the background of SRD-14 cells and deficient in both Insig-1 and Insig-2. In addition to the previous *Insig-1* gene defect, this cell line harbors a deletion of one allele of the *Insig-2* gene, and Insig-2 mRNA expression is reduced to less than 20% of wild-type cells. As a result of their combined deficiencies in Insig-1 and –2, SRD-15 cells are completely refractory to sterol-mediated actions on SREBP processing. Regulation is restored by transfecting cells with cDNAs encoding either of the two Insig isoforms, Insig-1 or Insig-2.

Taken together, the studies in mutant cell lines provide compelling genetic evidence for the importance of forming a functional sterol-sensing complex, which requires three membrane proteins: SREBP, Scap and Insig. Lacking any one of three components or having mutation in these proteins renders the cells resistant to sterols. More importantly, the functional sterol-sensing not only requires the presence of all three proteins, but also requires them to be expressed in an appropriate ratio to each other. Careful gene dosage studies in cultured cells revealed that only within a narrow window of the Scap/Insig stoichiometry does the system respond to sterol regulation. Overexpression of Insig-1 or –2 by transfection causes a marked leftward shift in inhibition of SREBP cleavage, reflecting the process much more sensitive to sterols (Yang et al., 2002; Yabe et al., 2002). When expressed at extremely high levels, Insig-1 can trap the Scap/SREBP complex in the ER, even without the addition of exogenous sterols. Conversely, when Scap is in molar excess compare to Insig, SREBP processing is insensitive to sterols as mentioned earlier. In conclusion, Insigs, along with Scap/SREBP, are the central players in regulating cholesterol homeostasis.

Latest studies suggest that cholesterol and its hydroxylated derivative, 25-hydroxycholesterol (25-HC) employ different mechanisms to inhibit ER-to-Golgi transport of Scap. This conclusion is drawn from several lines of evidence. First, through the use of trypsin cleavage assay, Scap is shown to undergo a conformational change when cholesterol is added to intact cells or ER membranes. Once in its cholesterol bound conformation, Scap binds to Insig proteins, and remains in the ER along with its attached SREBP (Brown et al., 2002; Adams et al., 2003, 2004). Second, through the use of in vitro binding assay, Scap is shown to bind specifically to [^{3}H] cholesterol in a saturable kinetics (Radhakrishnan et al., 2004). In these experiments, purified recombinant membrane domain of Scap (TM1-8) behaved like a standard receptor for cholesterol when it was mixed with [^{3}H] cholesterol in detergent micelles. Finally, in contrast to cholesterol, 25-hydroxycholesterol (25-HC), a more potent inhibitor of SREBP processing, neither binds Scap directly nor induces a conformational change in Scap when added to membranes *in vitro* (Adams et al., 2004; Radhakrishnan et al., 2004). However, it still induced Scap to bind to Insigs, as revealed by altered migration of the complex on blue native gel electrophoresis (Yang et al., 2002). Thus, to exert its inhibitory action on SREBP processing, this oxysterol must interact with an unidentified receptor-like protein that enhances Insig-Scap binding with no detectable conformational changes in Scap.

Scope of the current study

The aim of this study is to further characterize the role of Insig-1 in the feedback regulation of cholesterol homeostasis.

In Chapter 2 of this thesis, I describe the results of sterol-induced complex formation between Insig-1 and Scap by blue-native polyacrylamide gel electrophoresis (BN-PAGE) and coimmunoprecipitation. In addition, I report an important role for Asp-205, a conserved amino acid located at the beginning of the fourth loop of Insig-1. Mutations that abolish this negative charge produced an inactive Insig-1 that no longer binds to Scap and fails to degrade HMG CoA reductase in the presence of sterols.

In Chapter 3 of this thesis, I disclose the finding of a sterol-regulated ubiquitination and degradation of Insig-1. In sterol-depleted cells, Insig-1 is rapidly ubiquitinated on lysines 156 and 158 and degraded in proteasomes. Sterol-induced binding of Insig-1 to Scap prevents Insig-1 ubiquitination and degradation. Along with the transcriptional regulation of Insig-1 mRNA, the dynamic change of Insig-1 stability creates a convergent mechanism for feedback control of cholesterol synthesis and uptake.

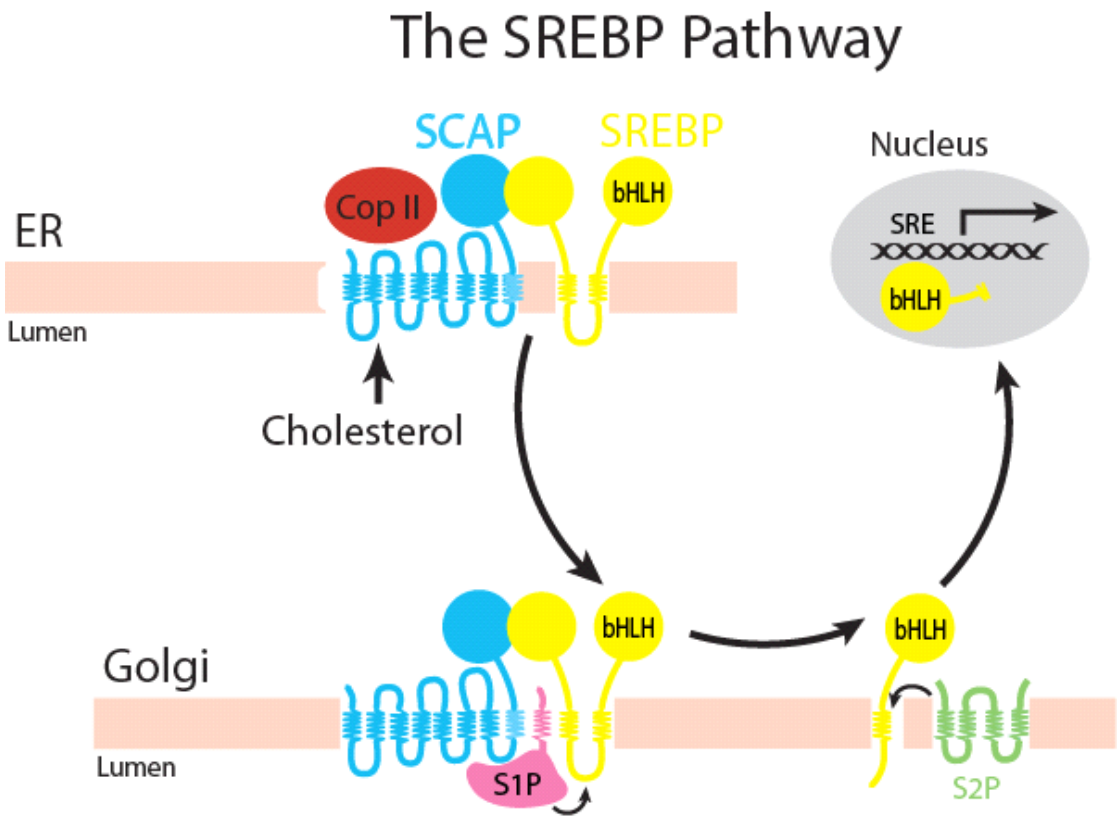
The SREBP Pathway
SCAP
SREBP
Nucleus
Cop II
bHLH
ER
SRE
bHLH
Lumen
Cholesterol
bHLH
bHLH
Golgi
Lumen
S1P
S2P

Figure 1-1

CHAPTER 2 ASP-205 IN INSIG-1 IS ESSENTIAL FOR ITS BINDING TO SCAP

Results

Sterol induced complex formation between Insig-1 and Scap

The experiment in Figure 2-1 demonstrated a native complex formation between Insig-1 and Scap using the technique of blue native-polyacrylamide gel electrophoresis (BN-PAGE), which was developed by Schagger et al. (1994) for the resolution of membrane proteins. SRD 13A cells, a line of CHO cells that lacks Scap owing to mutations in both copies of the gene (Rawson et al., 1999), were transfected with a plasmid encoding Myc-tagged Insig-1. Isolated membranes were solubilized with digitonin, and the supernatants were treated with Commassie blue, which imparts a negative charge, and 6-amino-n-hexanoic acid, which helps to keep the proteins in solution. After electrophoresis in a discontinuous solvent system, the proteins were transferred to a PVDF membrane and incubated with an antibody against the Myc tag on Insig-1. As shown in Figure 2-1A, free Insig-1 is visualized as a primary band (designated unbound Insig-1 in Figure) and a diffuse tail that extends upward in the gel (lane 1). This pattern was not affected by sterols in the absence of Scap (lane 2). When Scap was co-expressed, the amount of unbound Insig-1 was partially reduced, and a discrete band was revealed at a higher position (designated Scap/Insig-1 complex; lane 3). The addition of sterols caused a complete disappearance of unbound Insig-1 and a further increase in the Scap/Insig-1 complex (lane 4).

To show that the complex contained Scap as well as Insig-1, an antibody supershift experiment was performed. Digitonin-solubilized extracts were prepared from sterol-treated cells and incubated with an antibody against Scap prior to electrophoresis (Figure 2-1A, lanes 5–8). In the absence of Scap cotransfection, the anti-Scap antibody had no effect on the migration of unbound Insig-1 (lanes 5 and 6). When Scap was overexpressed, the band designated Scap/Insig-1 complex was detected as previously, and its migration was not affected when the extracts were incubated with a control monoclonal antibody (lane 7). However, when the extracts were incubated with the anti-Scap antibody, the complex migrated more slowly on the gel (supershifted complex in lane 8). These data indicate that Insig-1 forms a complex with Scap and that the formation of the complex is enhanced by sterols.

The coimmunoprecipitation (IP) experiment of Figure 2-1B further confirms that Insig-1 binds to Scap only in the presence of sterols. Extracts of transfected cells were subjected to immunoprecipitation with an antibody against the Myc epitope on Insig-1. Pellets and supernatants were subjected to SDS-PAGE and blotted with various antibodies (Figure 2-1B). In the absence of sterols, there was no precipitation of Scap (lanes 4 and 6). When sterols were present, Scap coprecipitated with Insig-1, and the amount of Scap in the immunoprecipitate increased proportionally to its expression level.

Asp-205 in Insig-1 is essential for its binding to Scap

To further understand the structure basis of sterol regulated Scap-Insig interaction, a site-directed mutagenesis approach was performed to look for residues that are critical for Scap/Insig-1 complex formation. Figure 2-2 shows the amino acid sequence and

membrane topology of human Insig-1. Residues that are identical in Insig-1 sequences from 9 animal species are indicated in black. In an initial attempt to identify functionally important residues, I prepared plasmids encoding mutant Insigs in which the conserved residues were changed individually to alanine. The plasmids were introduced into SRD 13A cells together with epitope-tagged SREBP-2 and Scap. The transfected cells were assayed for the ability of the mutant Insig-1 to support processing of SREBP-2 in the presence of 25-HC. These preliminary studies revealed an important function for Asp-205, which is located at the beginning of the fourth loop of human Insig-1. This residue is conserved in all animal species examined.

In the experiment shown in Figure 2-3, SRD 13A cells were transfected with cDNAs encoding either wild-type or mutant Insig-1 under control of the strong CMV promoter, together with a plasmid encoding epitope-tagged SREBP-2 and Scap. Cells were incubated in the absence or presence of sterols for 5 hrs. Total cell extracts were analyzed by SDS-PAGE and immunoblotting with various antibodies. When Scap was over-expressed, the full-length precursor form as well as the nuclear form of SREBP-2 was observed. Addition of sterols did not affect the amount of the nuclear form (Figure 2-3, lanes 1 and 2), indicating that the retention process was saturated by the excess Scap. Increasing level of wild-type Insig-1 expression restored sterol regulated SREBP-2 processing as previously reported (lanes 3-8). However, over-expression of mutant Insig-1 (D205A) up to highest level (0.2 μg of plasmid) failed to inhibit SREBP-2 processing when sterols were added (lanes 13 and 14). These results suggest that the point mutation at position 205 of Insig-1 fails to inhibit the transport of Scap/SREBP complex from ER to Golgi.

For Scap/SREBP complex to be retained in the ER, Scap must bind to Insig when cellular cholesterol level is high. To address whether the D205A mutation interferes with the binding between Insig-1 and Scap, coimmunoprecipitation experiments were performed (Figure 2-4A). When Myc-tagged Insig-1 was expressed alone in SRD 13A cells, no complex with Scap was observed (Figure 2-4A, lanes 2 and 3). Co-expression with Scap produced a Scap/Insig-1 complex in the presence of sterols (lane 5), but disappeared upon sterol depletion (lane 4). In marked contrast, mutant Insig-1 (D205A) did not form a complex with Scap under either condition (lanes 6 and 7).

To test whether the D205A mutation specifically blocks the interaction with Scap, or whether it affects the global folding of the protein, I did a similar experiment examining the complex formation between Insig-1 and VAP-A or VAP-B, which were identified as Insig-1 associated proteins in multiple purification trials (Yang et al., 2002). CHO cells were transfected with HA-tagged VAP-A or VAP-B along with Myc-tagged Insig-1. Cell extracts were subjected to immunoprecipitation with an antibody against the HA epitope on VAP-A or VAP-B. As shown in Figure 2-4B, wild-type and mutant D205A Inisg-1 were immunoprecipitated equally well with VAP-A or VAP-B (lanes 5-8), indicating that reduced interaction between Scap and D205A Insig-1 is unlikely caused by denaturation or unfolding of the mutant protein.

Asp-205 in Insig-1 is required for HMG CoA reductase degradation

Since Insig-1 is also involved in sterol-mediated degradation of HMG CoA reductase, I next examine the effect of Insig-1 (D205A) on reductase degradation. For this purpose, wild-type or mutant version of Insig-1 was transfected into CHO-K1 cells together with a

plasmid encoding a truncated version of HMG CoA Reductase containing the entire membrane anchor domain (TM1-8) under control of the CMV promoter. Cells were incubated with or without sterols plus mevalonate for 5 hrs, and subjected to immunoblot analysis. As expected, in the absence of Insig-1, the amount of reductase did not change when sterols and mevalonate were added (Figure 2-5A, lanes 1 and 2), suggesting that over-expressed reductase had saturated a protein necessary for sterol-accelerated degradation. 10 ng of wild-type Insig-1 co-transfection was able to degrade some reductase in the presence of sterols and mevalonate (lanes 3 and 4). At higher Insig-1 levels, the reductase was completely disappeared at the same condition (lanes 5 and 6). However, co-transfection of mutant D205A Insig-1 failed to induce reductase degradation even when the mutant protein was expressed 5 to 10 fold higher than wild-type protein (lanes 7-12).

In a similar experiment, sterol stimulated ubiquitination of reductase was tested. CHO-K1 cells were transfected with either wild-type or mutant Insig-1, and T7- tagged HMG CoA reductase. To enhance sensitivity of ubiquitin detection, pEF1a-HA-ubiquitin, an expression plasmid encoding human ubiquitin with an NH2 terminal tag consisting of two copies of the HA epitope was also cotransfected. After treatment for 2 hr with MG-132, cells were harvested, transfected reductase was immunoisolated from detergent lysates with anti-T7 agarose beads, and samples were subjected to SDS-PAGE. In the result shown in Figure 2-5B, immunoblot analysis with anti-HA revealed that wild-type Insig-1 facilitated reductase ubiquitination in the presence of sterols plus mevalonate (Figure 2-5B, lanes5 and 6). Mutating aspartic acid 205 to alanine abolished the wild-type function in sterol-regulated ubiquitination of reductase (lanes 7-10). Considered

together, the results of Figure 2-5 suggest that the aspartic acid 205 which lies at the beginning of the fourth loop of Insig-1 is not only important in ER retention of the Insig-1/Scap/SREBP complex, but also in sterol-dependent ubiquitination and degradation of HMG CoA reductase.

Insig-1 and -2 proteins are functionally similar in Scap/SREBP pathway and reductase degradation in cultured cells. Amino acid alignment between these two proteins shows the aspartic acid residue is conserved in both Insig-1 and -2 (Figure 2-2). To address whether this aspartic acid residue is also essential in Insig-2 mediated activities, I mutated the aspartic acid at position 149 in Insig-2 (D149A) which corresponds to the Asp-205 residue in Insig-1 to alanine, and tested its effects on both SREBP-2 cleavage and reductase degradation (Figure 2-5). SRD 13A cells were transfected with cDNAs encoding HSV-tagged SREBP-2, Scap, wild-type or mutant Insig-2. Cells were incubated in the absence or presence of sterols and harvested for measurement of the amounts of nuclear SREBP-2. Overproduction of Scap without Insig-2 led to non-regulated SREBP-2 processing (Figure 2-6A, lanes 1 and 2). Co-expression of wild-type Insig-2 restored sterol mediated suppression of the SREBP-2 cleavage (lanes 3 and 4). Low or equal levels of Insig-2 (D149A) were not able to completely inhibit SREBP-2 processing when sterols were added (lanes 5-8). At the highest expression level (3μg), there was some suppression by sterols (lanes 9 and 10), but the effect was much less complete than observed in wild-type case.

To test the effect of the D149A mutation in Insig-2 on regulated reductase degradation, wild-type or mutant version of pCMV-Insig-2-Myc together with pCMV-HMG-Red (TM1-8)-T7 were transfected into CHO-K1 cells. After 5 hr treatment of

sterols plus mevalonate, cells were harvested, and transfected reductase was analyzed by immunoblotting with anti-T7 antibody. Consistent with the earlier data, only wild-type Insig-2 led to the disappearance of reductase when cells were incubated with sterols and mevalonate (Figure 2-6B, lanes 3 and 4). The D149A mutation had no effect at all levels examined (lanes 5-10). Together, the results of Figure 2-6 strengthen the view that the conserved aspartic acid in both Insig-1 and -2 is essential for the ability of Insigs to mediate the retention of the Scap/SREBP complex in the ER and the regulated degradation of HMG CoA reductase.

The negative charge at position 205 in Insig-1 is involved in complex formation

To determine whether the defect in Insig-1 (D205A) is due to the loss of the negative charge, I prepared plasmids encoding Insig-1 with substitutions with either similar charge glutamic acid or opposite charge arginine at this position and transfected them into SRD 13A cells (Figure 2-7). When Scap was over-expressed without Insig-1, SREBP-2 cleavage was not regulated by sterols (Figure 19, lanes 1 and 2). Co-expression of wild-type Insig-1 restored sterol regulation of SREBP-2 processing (lanes 3 and 4). Substitution of glutamic acid for aspartic acid preserved most of the ability of wild-type Insig-1 to block SREBP-2 cleavage in the presence of sterols (lanes 5-8). Substitution with opposite charge arginine with two different levels destroyed this function (lanes 9-12). Considered together, these data suggest that Insig-1 requires a negatively charged amino acid at position 205 to bind to Scap in the presence of 25-HC.

Discussion

Insig-1 was both identified as a target gene of nSREBPs and the limiting factor for ER retention of the Scap/SREBP complex from Brown and Goldstein' laboratory (Luong, 2000; Yang et al., 2002). In 1998, by using subtractive cDNA hybridization Insig-1 mRNA was shown to be up-regulated in livers of transgenic mice that overexpressed an active version of SREBP-1a and SREBP-2. Subsequent characterization further proved that Insig-1 mRNA level is regulated in parallel with nSREBPs under conditions of both sterol deprivation and repletion. Here, through the use of BN-PAGE, I show the formation of a complex between Insig-1 and Scap. As observed in Figure 2-1A, free Insig-1 migrates to the bottom of the gel. Co-expression of Scap causes a retardation of Insig-1 migration to a new position. This retardation reflects the formation of a Scap/Insig-1 complex as revealed by the further retardation of the complex by incubation with anti-SCAP (Figure 2-1A, lane 8). The amount of the complex is increased and unbound Insig-1 disappears when the cells are treated with sterols under conditions in which the Scap/SREBP complex is retained in the ER (Figure 2-1A, lane 4).

In the current studies, I also disclose a functional role for the universally conversed negatively charged aspartic acid at the membrane interface of Insig-1. When Asp-205 is changed to alanine, Insig-1 decreases binding to Scap in the presence of sterols (Figure 2-4A). The resulting loss of retention complex leads to constitutive SREBP processing and activation of the target genes (Figure 2-3). In contrast, this mutant still binds normally with other Insig-1 interacting proteins, including VAP-A and VAP-B, suggesting that the mutation does not lead to global protein denaturation or unfolding (Figure 2-4B).

Both Scap and HMG CoA reductase bind to Insigs in a sterol-dependent fashion by virtue of their shared sterol-sensing domains. The results in Figure 2-5 further confirmed that Scap and reductase interact with the same site on Insig-1, as revealed by the fact that Insig-1 (D205A) also failed to ubiquitinate and degrade reductase in the presence of sterols. However, the mechanism by which binding to the same Insigs can have such different consequences is currently unknown. Hopefully, this question will be answered with new identification of other members that are differentially involved in either complex. Moreover, there are three other proteins that share the sequence homology of the sterol-sensing domain: Niemann-Pick C1 protein, which participates in the intracellular movement of cholesterol; Patched, the receptor for Hedgehog, a protein that contains covalently bound cholesterol; and Niemann-Pick C1-like protein (NPC1L1), which functions in the intestinal absorption of cholesterol. It is tempting to speculate that these proteins also bind to Insig-1 in a sterol-dependent manner. If so, then the question of whether the D205A mutant can interfere with these individual complex remains to be determined.

Currently, we know that cholesterol and 25-HC act differently in terms of sterol sensing. Cholesterol can directly bind to Scap protein and change its conformation to facilitate the binding to Insig-1, while 25-HC does not interact with Scap, and requires other proteins to participate the complex formation in the presence of the oxysterol. In this initial study, I did not separate the effects of cholesterol and 25-HC on Insig-1 mediated SREBP processing and HMG CoA reductase degradation. So it will be interesting to test whether this point mutation can preferentially affect one sterol but not the other.

Material and Methods

Materials

We obtained MG-132, digitonin and nonidet P-40 from Cal Biochem; cycloheximide from Sigma; all sterols from Steraloids, Inc.; hydroxypropyl-β-cyclodextrin from Cyclodextrin Technologies Development, Inc.; Lipoprotein-deficient newborn calf serum (d > 1.215 g/ml) was prepared by ultracentrifugation (Goldstein, J. L., Basu, S. K., and Brown, M. S. (1983) *Methods Enzymol.*). Solutions of sodium compactin, sodium mevalonate, and sodium oleate were prepared as described (Kita et al., 1980; Hannah et al., 2001).

Antibodies

We obtained horseradish peroxidase-conjugated, donkey anti-mouse, and anti-rabbit IgGs (affinity-purified) from Jackson Immunoresearch Laboratories; monoclonal anti-HSV-Tag antibody (IgG) and monoclonal anti-T7 antibody (IgG) from Novagen; polyclonal anti-HA IgG from Santa Cruz Biotechnology, Inc.; polyclonal anti-Myc and anti-T7 IgGs from Bethyl Laboratories; and cells producing IgG-9E10, a mouse monoclonal antibody against Myc tag, from American Type Culture Collection. IgG-7D4, a mouse monoclonal antibody against hamster SREBP-2 (Sakai et al., 1996); IgG-1D2, a mouse monoclonal antibody against human SREBP2 (Yabe et al., 2002); IgG-9D5, a mouse monoclonal antibody against hamster Scap (Sakai et al., 1997); and IgG-R139, a rabbit polyclonal antibody against hamster Scap (Sakai et al., 1997), were previously described in the indicated references.

Plasmid Constructs

The following recombinant plasmids have been described: pEF1a-HA-ubiquitin (provided by Dr. Zhijian Chen, University of Texas Southwestern Medical Center), encoding amino acids 1-76 of human ubiquitin preceded by an epitope tag derived from the influenza hemagglutinin (HA) protein (YPYDVPDY) under the control of the EF1a promoter (Kanayama et al., 2004); pCMV-Insig-1-Myc, encoding human Insig-1 followed by six tandem copies of a c-Myc epitope tag under control of the cytomegalovirus (CMV) promoter (Yang et al., Cell); pCMV-Insig-2-Myc, encoding human Insig-2 followed by six tandem copies of a c-Myc epitope tag under control of the cytomegalovirus (CMV) promoter (Yabe et al., 2002); pCMV-Scap, encoding wild-type hamster Scap under control of CMV promoter (Sakai et al., 1997); pCMV-HMG-Red-T7, encoding full-length hamster reductase (amino acids 1–887) followed by three tandem copies of the T7-epitope tag (MASMTGGQQMG) under control of CMV promoter (Sever et al., 2003); pCMV-HMG-Red (TM1-8)-T7, encoding amino acids 1–346 of hamster HMG-CoA reductase followed by three tandem copies of the T7 epitope tag (MASMTGGQQMG) under control of CMV promoter (Sever et al., 2003); pCMV-VAP-A-HA and pCMV-VAP-B-HA (provided by Joon No Lee) are generated as follows: Full-length human VAP-A cDNA in pBluescript SK2 (Id No. 328880) and VAP-B (Id No. 75005) were obtained from the IMAGE Consortium (LLNL; Research Genetics Inc., Huntsville, AL). pCMV-VAP-A-HA encodes amino acids 1-242 of human VAP-A followed by three tandem copies of a HA epitope tag under control of CMV promoter. A BamHI-NheI fragment containing the full coding sequence of the human VAP-A was amplified by PCR and inserted into pCDNA3.1 with the HA epitope tag. pCMV-VAP-B-HA (amino acids 1-243) encodes amino acids 1-243 of human VAP-B followed by

three tandem copies of a HA epitope tag under control of CMV promoter. The plasmid for VAP-B was made by the same method of VAP-A. Integrity of pCMV-VAP-A-HA and pCMV-VAP-B-HA was confirmed by sequencing the entire coding region and the ligation joints. pCMV-Insig-1(D205A)-Myc, pCMV-Insig-1(D205E)-Myc, pCMV-Insig-1(D205R)-Myc, and pCMV-Insig-2 (D149A)-Myc were generated by site-directed mutagenesis using the QuikChange site-directed mutagenesis kit (Stratagene). The coding regions of all plasmids were sequenced before use.

Tissue Culture Media

Medium A contains a 1:1 mixture of Ham's F-12 medium and Dulbecco's modified Eagle's medium supplemented with 100 units/ml penicillin and 100 μg/ml streptomycin sulfate. Medium B contains medium A supplemented with 5% (v/v) newborn calf lipoprotein-deficient serum, 50 μM sodium compactin and 50μM sodium mevalonate. Medium C contains medium A supplemented with 5% (v/v) fetal calf serum, 5 μg/ml cholesterol, 1 mM sodium mevalonate, and 20 μM sodium oleate.

Cell Culture

Cells were maintained in monolayer culture at 37 °C in 8–9% CO_2. CHO-7 cells are a clone of CHO-K1 cells selected for growth in lipoprotein-deficient serum (Metherall et al., 1989). SRD-13A cells ($Scap^{-/-}$) are mutant cells derived from CHO-7 cells (Rawson et al., 1999).

Stock cultures of CHO-K1 cells were maintained in medium A supplemented with 5% (v/v) fetal calf serum (FCS). CHO-7 cells were maintained in medium A

supplemented with 5% (v/v) newborn calf lipoprotein-deficient serum. SRD-13A cells were maintained in medium C.

Transient Transfection of Cells

CHO-K1, CHO-7 and SRD-13A cells were transiently transfected with FuGENE 6 reagent (Roche Applied Science) according to the manufacturer's protocol. The total amount of DNA in each transfection was adjusted to 3 μg per dish by addition of pcDNA3 mock vector. Conditions of incubation after transfection are described in the Figure legends. At the end of the incubation, duplicate dishes of cells for each variable were harvested and pooled for analysis.

Cell Fractionation and Immunoblot Analysis

The pooled cell pellets from duplicate dishes of cells were resuspended in 0.5 ml of buffer (10 mM HEPES-KOH [pH 7.6], 10 mM KCl, 1.5 mM $MgCl_2$) supplemented with protease inhibitor cocktail consisting of 10 μg/ml leupeptin, 5 μg/ml pepstatin A, 25 μg/ml ALLN, and 2 μg/ml aprotinin. The cell suspension was passed through a 22.5 gauge needle 30 times and centrifuged at 1000 × g for 5 min at 4°C, the nuclear extracts and membrane fractions were prepared as describes previously(Sakai et al., 1996). To prepare a whole-cell lysate fraction, cell pellets from duplicate dishes were resuspended in 0.2 ml of buffer (50 mM HEPES-KOH [pH 7.6], 100 mM NaCl, 1.5 mM $MgCl_2$, 1% NP-40, and protease inhibitor cocktail consisting of 10 μg/ml leupeptin, 5 μg/ml pepstatin A, 25 μg/ml ALLN, and 2 μg/ml aprotinin), rotated at 4°C for 30 min, and centrifuged at 20,000g for 20 min at 4°C. The supernatant from this spin was mixed with

5X SDS loading buffer(150 mM Tris-Cl at ph 6.8, 15% SDS, 25% (v/v) glycerol, 0.02% (w/v) bromophenol blue, and 12.5% (v/v) 2-mercaptoethanol).

All fractions were subjected to SDS-PAGE and immunoblot analysis as previously described (Sakai et al., 1996). The primary antibodies used for immunoblotting are given in the Figure legends. Secondary antibodies were horseradish peroxidase-conjugated donkey anti-mouse and anti-rabbit IgGs (1: 5000 dilution). Bound secondary antibodies were visualized by chemiluminescence using the SuperSignal substrate system (Pierce) according to the manufacturer's instructions. Filters were exposed to Kodak X-Omat Blue XB-1 films at room temperature for indicated time.

Immunoprecipitation

The pooled cell pellets from duplicate dishes of cells were resuspended in 0.5 ml of buffer A (50 mM HEPES-KOH [pH 7.6], 100 mM NaCl, 1.5 mM $MgCl_2$, 0.1% NP-40, and protease inhibitors (see above)). Cell lysates were prepared and immunoprecipitation was performed as described (Sakai et al., 1997) with the following modifications. Precleared lysates were rotated for 16 h at 4°C with 20 µg of either control nonimmune IgG, polyclonal anti-Myc (40 µg/ml), and polyclonal anti-HA (40µg/ml) together with 50 µl of protein A/G agarose beads (Santa Cruz Biotechnology). After centrifugation, the resulting supernatants were mixed with 5X SDS loading buffer. The pelleted beads were washed three times(20 min each at 4°C) with 1 ml of buffer A; resuspended in 100 µl of buffer containing 10 mM Tris-HCl [pH 6.8], 1% (w/v) SDS, 100 mM NaCl and protease inhibitors; and mixed with 5X SDS loading buffer. Supernatants and pellets were boiled for 5 min, and subjected to SDS/PAGE and immunoblot analysis.

Blue Native-PAGE

Blue native-PAGE (BN-PAGE) was carried out as described by Schagger et al. (1994). A 16,000 *g* membrane pellet from transfected SRD-13A cells was isolated in buffer containing 50 mM HEPES-KOH [pH 7.2], 250 mM sorbitol, 70 mM potassium acetate, 5 mM sodium EGTA, and 1.5 mM magnesium acetate as described (Nohturfft et al., 2000). In the standard assay for detection of SCAP/INSIG-1 complex, aliquots of the membranes (50 μg protein in 100 μl) were mixed with 100 μl of buffer containing 40 mM HEPES-KOH [pH 7.0], 2 mM magnesium acetate, and 2% (w/v) digitonin in a final volume of 200 μl. After incubation at 4°C for 30 min, detergent-insoluble material was removed by centrifugation at 20,000 *g* for 2 min at 4°C. One aliquot of the supernatant (90 μl) was mixed with 10 μl of buffer containing 50 mM Bis-Tris-HCl [pH 7.0], 0.75 M 6-amino-n-hexanoic acid, 5% (w/v) Coomassie G250, and 10% (v/v) glycerol; loaded onto a 4%–16% BN gel; and subjected to PAGE (Schagger et al., 1994). After electrophoresis, proteins were transferred electrophoretically to a PVDF membrane (Millipore Corp.), destained with methanol, and subjected to immunoblot analysis with 0.33 μg/ml of polyclonal anti-Myc IgG directed against epitope-tagged INSIG-1. A separate 40 μl aliquot of the digitonin-containing supernatant was mixed with 10 μl of 5X Laemmli buffer and subjected to SDS-PAGE on 8% and 12% gels for immunoblot analysis of Scap and epitope-tagged Insig-1, respectively.

For antibody supershift assays, a 50 μl aliquot of membranes (10 μg) was added to 50 μl of the above digitonin-containing buffer together with 2 μg of monoclonal

antibody (control Ig-2001 or anti-Scap IgG-9D5, added in 2 μl). The mixture was incubated at 4°C for 30 min and processed for BN-PAGE.

Ubiquitination of HMG-CoA Reductase

Conditions of incubations are described in the Figure Legends. At the end of the incubation, cells were harvested, and immunoprecipitations with monoclonal anti-T7 IgG-coupled agarose beads (Novagen) against transfected reductase was carried out as described (Sever et al., 2003) with two modifications: the lysis buffer used to harvest the cells was supplemented with 10 mM N-ethylmaleimide and the pelleted beads were washed three times (30 min each). Immunoprecipitates were subjected to SDS-PAGE.

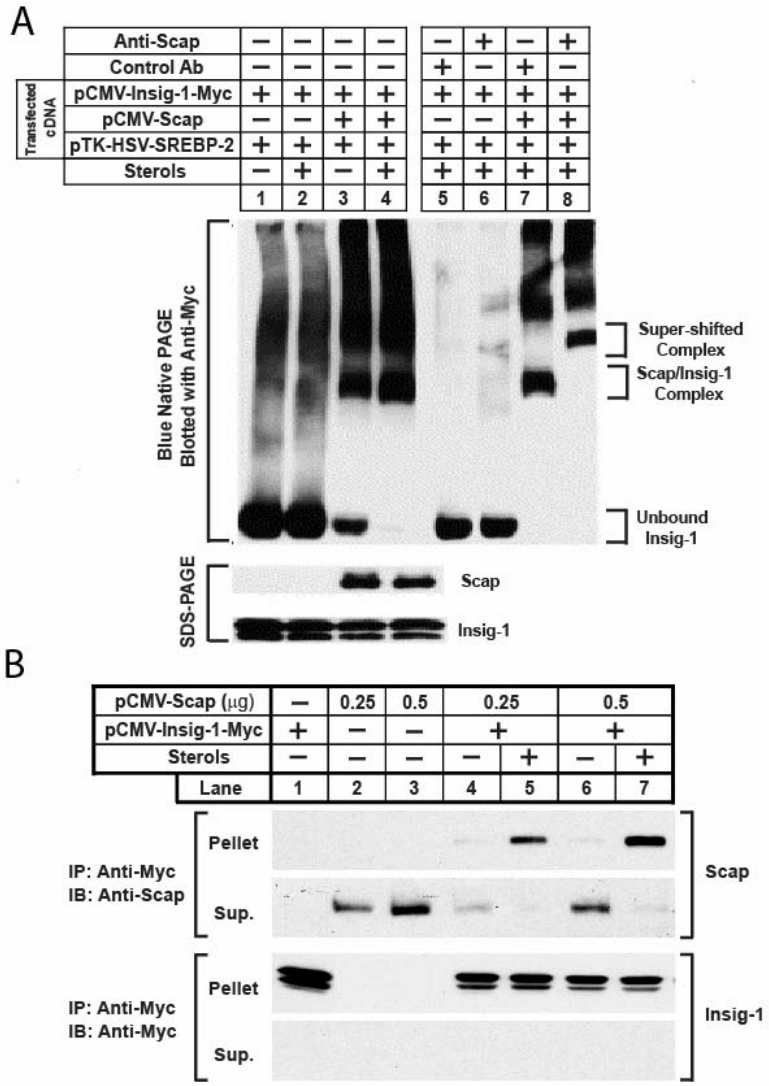
A
Anti-Scap
Control Ab
pCMV-Insig-1-Myc
pCMV-Scap
pTK-HSV-SREBP-2
Sterols
Transfected cDNA
1 2 3 4 5 6 7 8
Blue Native PAGE
Blotted with Anti-Myc
Super-shifted Complex
Scap/Insig-1 Complex
Unbound Insig-1
SDS-PAGE
Scap
Insig-1
B
pCMV-Scap (μg)
pCMV-Insig-1-Myc
Sterols
Lane
1 2 3 4 5 6 7
IP: Anti-Myc
IB: Anti-Scap
Pellet
Sup.
Scap
IP: Anti-Myc
IB: Anti-Myc
Pellet
Sup.
Insig-1

Figure 2-1

Figure 2-1 Sterol mediated Insig-1/Scap complex formation.

On day 0, SRD-13A cells were set up at 7×10^5 cells per 100 mm dish in medium C.

A) On day 2, the cells were transfected in medium A containing 5%FCS with the indicated plasmids as follows: 2 μg of pTK-HSV-SREBP-2; 4 μg of pCMV-Scap; and 60 ng of pCMV-Insig-1-Myc. 12 hr after transfection, cells were washed and switched to sterol-depleted medium B containing 1% HPCD. After incubation for 1 hr at 37°C, the cells were washed and switched to medium B in the absence (-) or presence (+) of 1 μg/ml of 25-HC plus 10 μg/ml of cholesterol (sterols). After incubation for 4 hr, cells from 4 dishes were pooled for measurement of Insig-1/Scap complex formation by BN-PAGE and immunoblot analysis as described in Experimental Procedures. In lanes 5–8, supershift assays were carried out with 2 μg control mouse monoclonal IgG-2001 (control Ab) (lanes 5 and 7) or 2 μg monoclonal anti-Scap IgG-9D5 (lanes 6 and 8). Filters were exposed to film for 1 s for lanes 1–4 and 15 s for lanes 5–8. Digitonin-solubilized extracts from lanes 1–4 were also subjected to SDS-PAGE and immunoblot analysis with 5 μg/ml of anti-Scap IgG-R139 or 0.33 μg/ml of polyclonal anti-Myc IgG (against Insig-1). Filters were exposed to films for 1 s.

B) On day 2, the cells were transfected in medium A containing 5% FCS with the indicated plasmids as follows: 0.1 μg of pCMV-Insig-1-Myc, and different amount of pCMV-Scap as indicated. 12 hr after transfection, cells were washed and switched to sterol-depleted medium B containing 1% HPCD. After incubation for 1 hr at 37°C, the cells were washed and switched to medium B in the absence (-) or presence (+) of 1 μg/ml of 25-HC plus 10 μg/ml of cholesterol (sterols). After incubation for 5 hr, cells were immunoprecipitated (IP) with 40 μg/ml polyclonal anti-Myc against Insig-1 as described in Experimental Procedures. Immunoprecipitated pellets (representing 0.25 dish of cells) and supernatants (representing 0.05 dish of cells) were subjected to SDS-PAGE and immunoblotted (IB) with 5 μg/ml of monoclonal IgG-9D5 (against Scap) and 1 μg/ml of anti-Myc monoclonal IgG (against Insig-1). Filters were exposed to film for 2-60s.

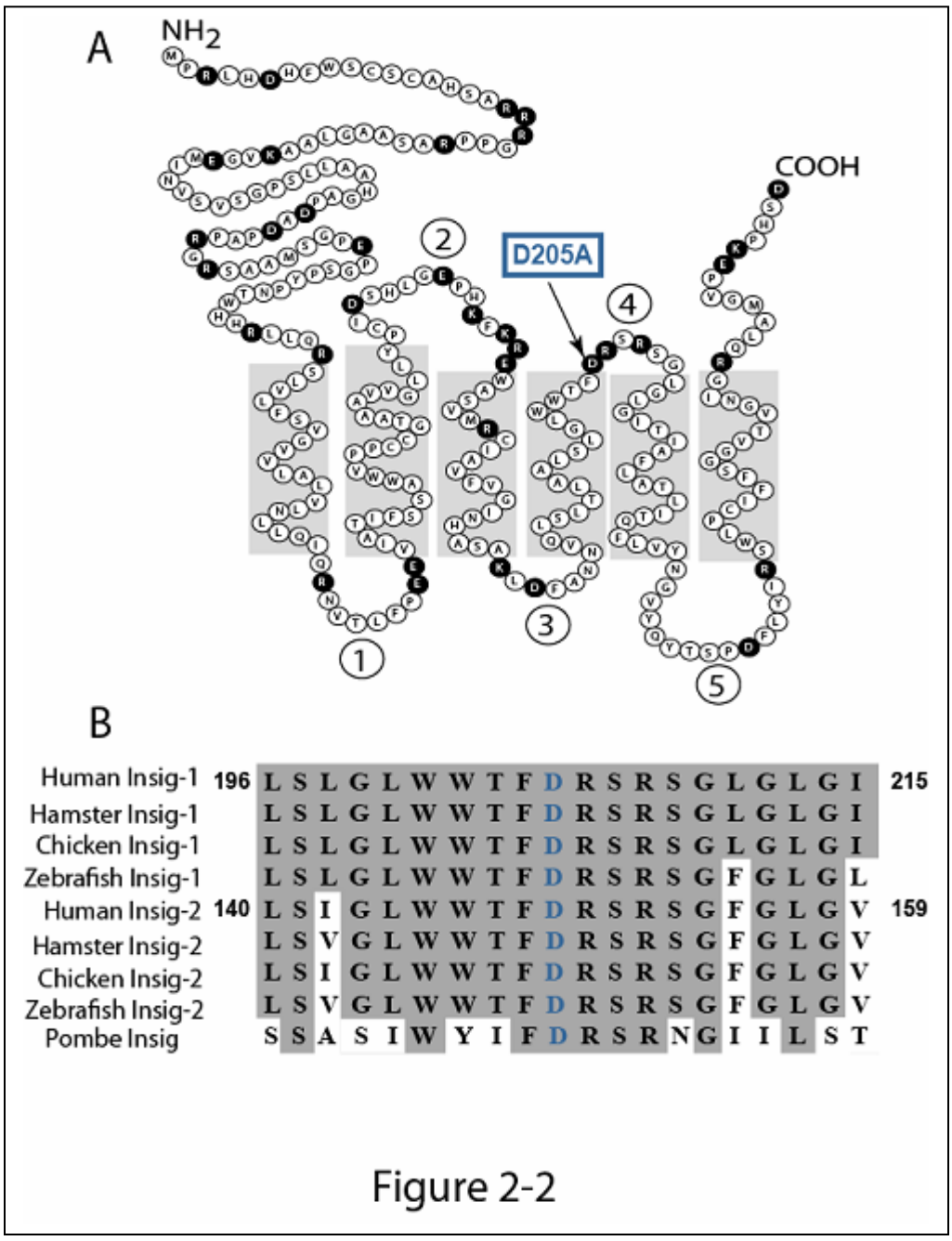
A
NH2
COOH
D205A
1
2
3
4
5
B
Human Insig-1 196 L S L G L W W T F D R S R S G L G L G I 215
Hamster Insig-1 L S L G L W W T F D R S R S G L G L G I
Chicken Insig-1 L S L G L W W T F D R S R S G L G L G I
Zebrafish Insig-1 L S L G L W W T F D R S R S G F G L G L
Human Insig-2 140 L S I G L W W T F D R S R S G F G L G V 159
Hamster Insig-2 L S V G L W W T F D R S R S G F G L G V
Chicken Insig-2 L S I G L W W T F D R S R S G F G L G V
Zebrafish Insig-2 L S V G L W W T F D R S R S G F G L G V
Pombe Insig S S A S I W Y I F D R S R N G I I L S T

Figure 2-2

Figure 2-2 Amino acid sequence and topology of Insig-1.

A) Topology of human Insig-1. Amino acids with positively or negatively charged side chains are shown in black.

B) Sequence alignment of Insig-1 by using the CLUSTALW program (DNASTAR, Madison, WI). Residues identical to human Insig-1 are shaded. GenBank accession numbers are as follows: AY112745 (human Insig-1); AF527628 (hamster Insig-1);NM_001030966 (chicken Insig-1); AF527626 (zebra fish Insig-1); AF527632 (human Insig-2); AF527629 (hamster Insig-2); NM_001031261 (chicken Insig-2); AF527627 (zebra fish Insig-2) and CAB41653 (Schizosaccharomyces pombe Insig).

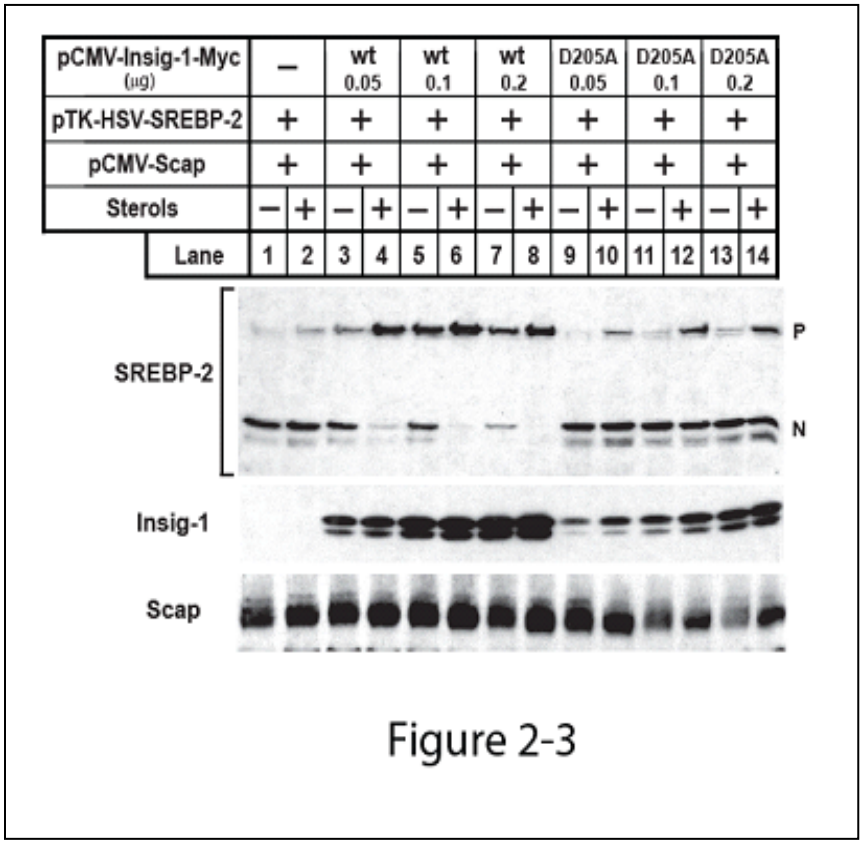
pCMV-Insig-1-Myc (μg)
–
wt 0.05
wt 0.1
wt 0.2
D205A 0.05
D205A 0.1
D205A 0.2
pTK-HSV-SREBP-2
pCMV-Scap
Sterols
Lane
1 2 3 4 5 6 7 8 9 10 11 12 13 14
SREBP-2
P
N
Insig-1
Scap

Figure 2-3

Figure 2-3 Mutant Insig-1 (D205A) is defective in mediating SREBP-2 processing.

On day 0, SRD-13A cells were set up at 3.5×10^5 cells per 60 mm dish in medium C. On day 2, cells were transfected in 3 ml of medium A containing 5% FCS with the following plasmids: 2μg of pTK-HSV-SREBP-2, 0.5μg of pCMV-Scap, the indicated amount of wild-type pCMV-Insig-1-Myc (wt) (lanes 3-8) or the D205A (lanes 9-14). The total DNA in each dish was adjusted to 3 μg by addition of pcDNA3 mock vector. On day 3, cells were switched to medium B containing 1% HPCD and incubated for 1 hr at 37°C. Cells were then washed twice with PBS and switched to medium B in the absence (-) or presence (+) of 1μg/ml 25-HC plus 10μg/ml of cholesterol (sterols). After incubation for 5 hr, cells were harvested, and whole cell lysates were subjected to SDS-PAGE and immunoblot analysis with IgG-9E10 (against Insig-1), IgG-R139 (against Scap), and anti-HSV tag antibody (against SREBP-2). P and N denote precursor and nuclear forms of SREBP-2, respectively. Filters were exposed to film for 5-30s.

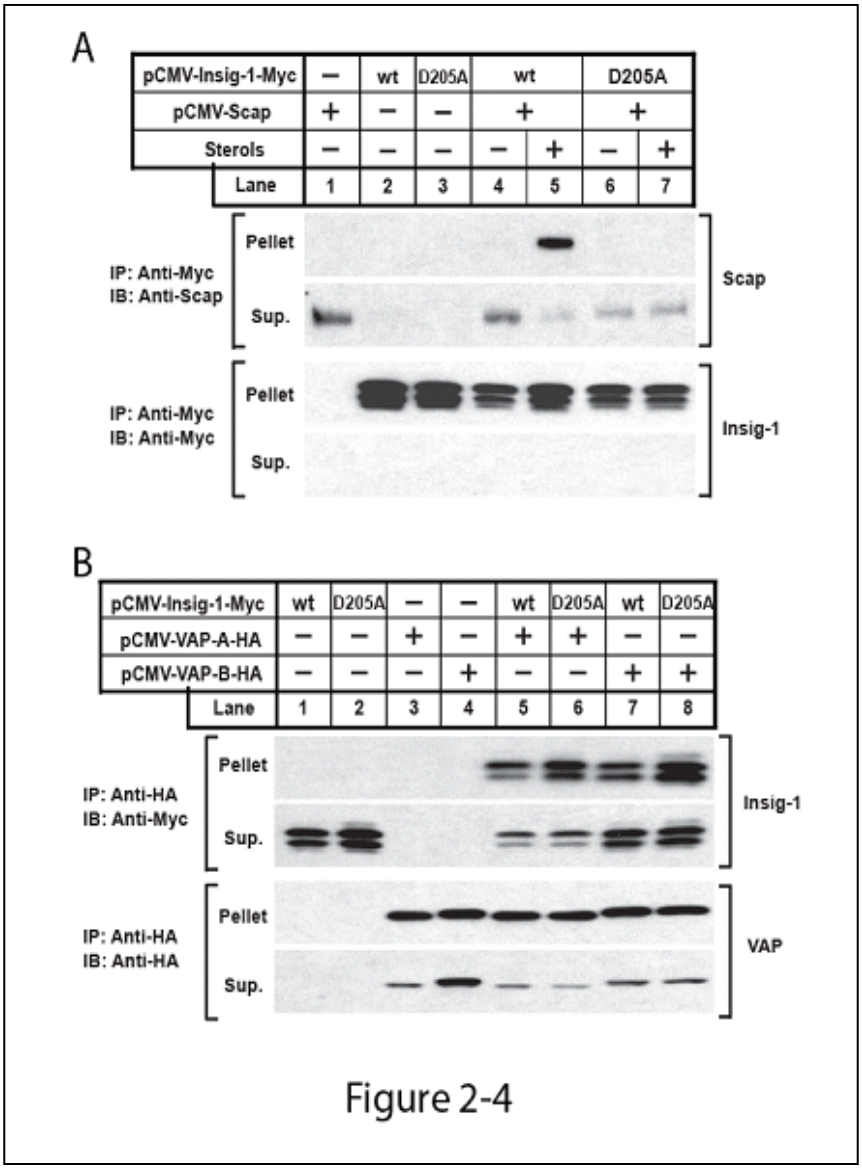
A
pCMV-Insig-1-Myc
pCMV-Scap
Sterols
Lane
wt
D205A
1 2 3 4 5 6 7
IP: Anti-Myc
IB: Anti-Scap
Pellet
Sup.
Scap
IP: Anti-Myc
IB: Anti-Myc
Insig-1
B
pCMV-Insig-1-Myc
pCMV-VAP-A-HA
pCMV-VAP-B-HA
1 2 3 4 5 6 7 8
IP: Anti-HA
IB: Anti-Myc
IP: Anti-HA
IB: Anti-HA
VAP

Figure 2-4

Figure 2-4 Reduced interaction of Insig-1 (D205A) with Scap proteins.

A) On day 0, SRD-13A cells were set up at 3.5×10^5 cells per 60 mm dish in medium C. On day 2, cells were transfected in 3 ml of medium A containing 5% FCS with the following plasmids: 0.25μg or 0.5μg of pCMV-Scap, 0.1 μg of wild-type pCMV-Insig1-Myc or the D205A. The total DNA in each dish was adjusted to 3μg dish by addition of pcDNA3 mock vector. Six hours after transfection, cells were refed with sterol-depleting medium B. After 16 hr, cells were switched to fresh medium B in the absence (-) or presence (+) of 1 μg/ml of 25-HC. After incubation for 5 hr, cells were immunoprecipitated (IP) with 40μg/ml polyclonal anti-Myc against Insig-1 as described in Experimental Procedures. Immunoprecipitated pellets (representing 0.25 dish of cells) and supernatants (representing 0.05 dish of cells) were subjected to SDS-PAGE and immunoblotted (IB) with 5 μg/ml of monoclonal IgG-9D5 (against Scap) and 1 μg/ml of anti-Myc monoclonal IgG (against Insig-1). Filters were exposed to film for 2-60s.

B) On day 0, CHO-7 cells were set up at 7×10^5 cells per 60 mm dish in medium A supplemented with 5% LPDS. On day 1, cells were transfected in 3 ml of medium A containing 5% FCS with the following plasmids: 1μg of pCMV-VAP-A-HA, 0.3μg of pCMV-VAP-B-HA, 0.1μg of wild-type pCMV-Insig1-Myc, and 0.2μg of the D205A. The total DNA in each dish was adjusted to 3μg dish by addition of pcDNA3 mock vector. After 16 hr, cells were immunoprecipitated (IP) with 20μg/ml polyclonal anti-HA against VAP-A or VAP-B as described in Experimental Procedures. Immunoprecipitated pellets (representing 0.25 dish of cells) and supernatants (representing 0.05 dish of cells) were subjected to SDS-PAGE and immunoblotted (IB) with 5 μg/ml of monoclonal IgG-9E10 (against Insig-1) and 1:2000 dilution of monoclonal anti-HA IgG (against VAP-A or VAP-B). Filters were exposed to film for 1-60s.

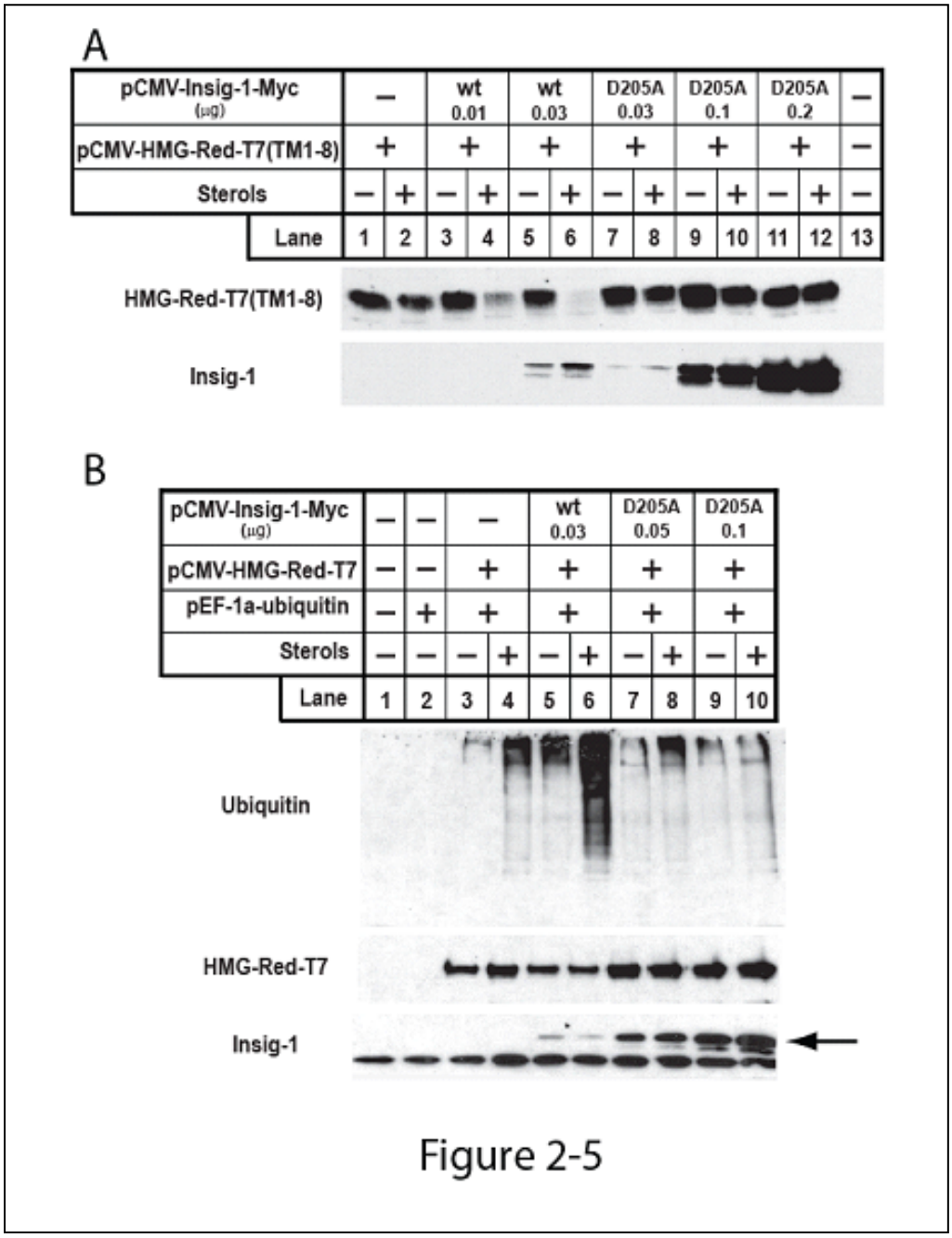
A
pCMV-Insig-1-Myc (μg)
–
wt 0.01
wt 0.03
D205A 0.03
D205A 0.1
D205A 0.2
–
pCMV-HMG-Red-T7(TM1-8)
+
+
+
+
+
+
–
Sterols
– + – + – + – + – + – + –
Lane
1 2 3 4 5 6 7 8 9 10 11 12 13
HMG-Red-T7(TM1-8)
Insig-1
B
pCMV-Insig-1-Myc (μg)
– – –
wt 0.03
D205A 0.05
D205A 0.1
pCMV-HMG-Red-T7
– – + + + +
pEF-1a-ubiquitin
– + + + + +
Sterols
– – – + – + – + – +
Lane
1 2 3 4 5 6 7 8 9 10
Ubiquitin
HMG-Red-T7
Insig-1

Figure 2-5

Figure 2-5 Mutant Insig-1 (D205A) is defective in sterol-mediated HMG CoA reductase ubiquitination and degradation.

On day 0, CHO-K1 cells were set up at 5×10^5 cells per 60 mm dish in medium A supplemented with 5% FCS. On day 1, cells were transfected in 2 ml of medium A containing 5% LPDS and 1μg of pCMV-HMG-Red (TM1-8)-T7 (A) or 1μg of pCMV-HMG-Red-T7 (B), the indicated amount of wild-type pCMV-Insig-1-Myc (wt) (lanes 3-6) or the D205A (lanes 7-12). In B, cells in each lane were also transfected with 0.1μg of pEF1a-HA-ubiquitin. Six hours after transfection, cells were refed with sterol-depleting medium B. After 16 hr, cells were switched to fresh medium B in the absence (-) or presence (+) of sterols (1 μg/ml of 25-HC plus 10mM mevalonate). In B, the medium also contained 10μM MG-132. After incubation for 5 hr, cells were harvested, membrane fractions were prepared as described in Experimental Procedures. Aliquots of the membrane extracts were subjected to SDS-PAGE and immunoblot analysis with monoclonal anti-T7-IgG (against HMG CoA reductase) and monoclonal IgG-9E10 (against Insig-1). Filters were exposed to film for 5-30 s. B, After incubation for 2 hr, cells were harvested, lysed, and subjected to immunoprecipitation with monoclonal anti-T7-coupled agarose beads. Aliquots of immunoprecipitates were subjected to SDS-PAGE and immunoblot analysis with polyclonal anti-HA-IgG (against ubiquitin), polyclonal anti-T7-IgG (against HMG CoA reductase) and polyclonal anti-Myc-IgG (against Insig-1). Filters were exposed to film for 5-60 s.

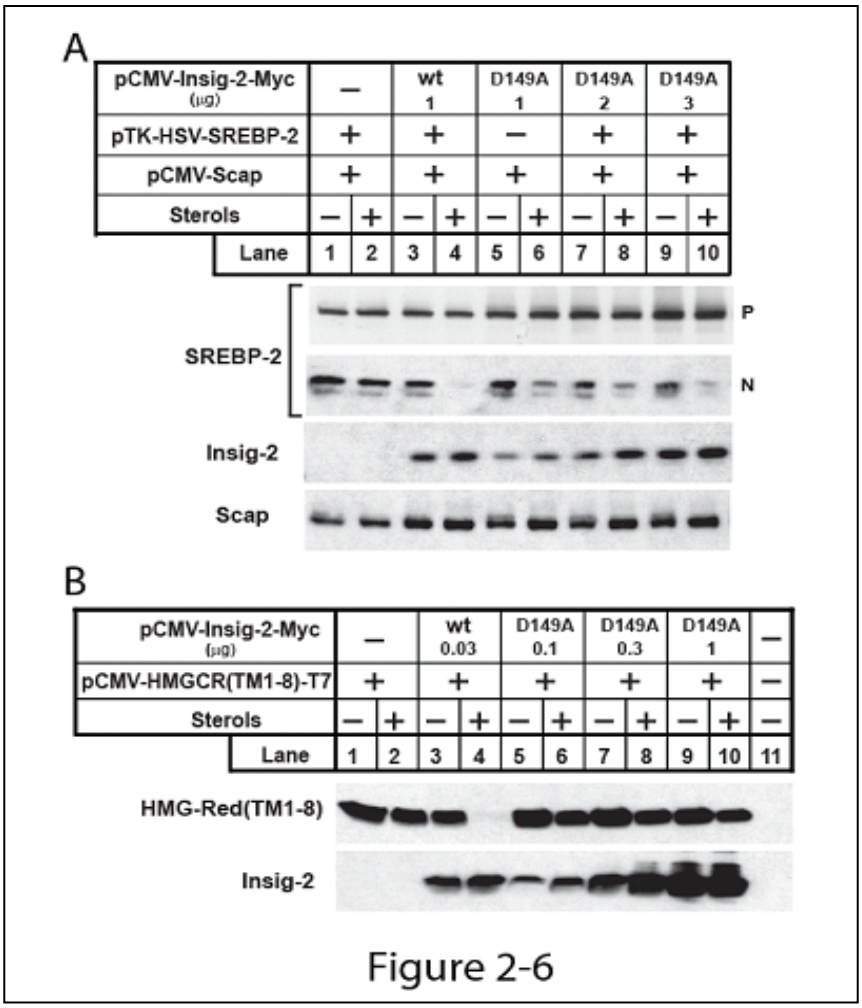
A
pCMV-Insig-2-Myc (μg)
–
wt 1
D149A 1
D149A 2
D149A 3
pTK-HSV-SREBP-2
pCMV-Scap
Sterols
Lane
1 2 3 4 5 6 7 8 9 10
SREBP-2
P
N
Insig-2
Scap
B
pCMV-Insig-2-Myc (μg)
wt 0.03
D149A 0.1
D149A 0.3
D149A 1
pCMV-HMGCR(TM1-8)-T7
1 2 3 4 5 6 7 8 9 10 11
HMG-Red(TM1-8)
Insig-2

Figure 2-6

Figure 2-6 Mutant Insig-2 (D149A) is defective in both SREBP-2 processing and reductase degradation.

A) On day 0, SRD-13A cells were set up at 3.5×10^5 cells per 60 mm dish in medium C. On day 2, cells were transfected in 3 ml of medium A containing 5% FCS with the following plasmids: 2μg of pTK-HSV-SREBP-2, 0.5μg of pCMV-Scap, the indicated amount of wild-type pCMV-Insig-2-Myc (wt) (lanes 3 and 4) or the D149A (lanes 5-10). The total DNA in each dish was adjusted to 3 μg by addition of pcDNA3 mock vector. On day 3, cells were switched to medium B containing 1% HPCD and incubated for 1 hr at 37°C. Cells were then washed twice with PBS and switched to medium B in the absence (-) or presence (+) of 1μg/ml 25-HC plus 10μg/ml of cholesterol (sterols). After incubation for 5 hr, cells were harvested, and whole cell lysates were subjected to SDS-PAGE and immunoblot analysis with IgG-9E10 (against Insig-2), IgG-R139 (against Scap), and anti-HSV tag antibody (against SREBP-2). P and N denote precursor and nuclear forms of SREBP-2, respectively. Filters were exposed to film for 1-60s.

B) On day 0, CHO-K1 cells were set up at 5×10^5 cells per 60 mm dish in medium A supplemented with 5% FCS. On day 1, cells were transfected in 2 ml of medium A containing 5%LPDS and 1μg of pCMV-HMG-Red (TM1-8)-T7, the indicated amount of wild-type pCMV-Insig-1-Myc (wt) (lanes 3-6) or the D205A (lanes 7-12). Six hours after transfection, cells were refed with sterol-depleting medium B. After 16 hr, cells were switched to fresh medium B in the absence (-) or presence (+) of sterols (1 μg/ml of 25-HC plus 10mM mevalonate) After incubation for 5 hr, cells were harvested, membrane fractions were prepared as described in Experimental Procedures. Aliquots of the membrane extracts were subjected to SDS-PAGE and immunoblot analysis with monoclonal anti-T7-IgG (against HMG CoA reductase) and monoclonal IgG-9E10 (against Insig-2). Filters were exposed to film for 3-30 s.

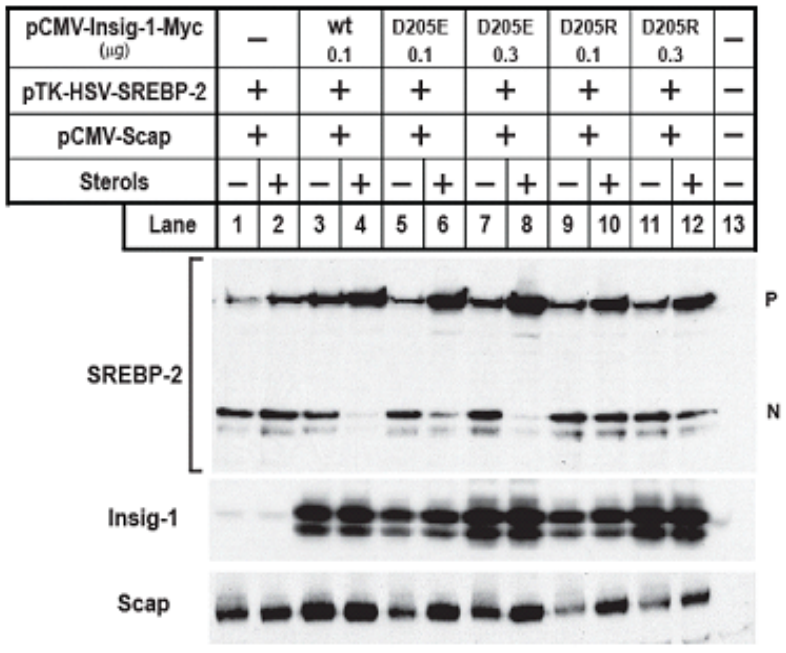
pCMV-Insig-1-Myc (μg)
–
wt 0.1
D205E 0.1
D205E 0.3
D205R 0.1
D205R 0.3
–
pTK-HSV-SREBP-2
+
+
+
+
+
+
–
pCMV-Scap
+
+
+
+
+
+
–
Sterols
– + – + – + – + – + – + –
Lane
1 2 3 4 5 6 7 8 9 10 11 12 13
SREBP-2
P
N
Insig-1
Scap

Figure 2-7

Figure 2-7 Effect of amino acid substitutions at residue 205 on Insig-1's facilitation of SREBP-2 cleavage.

On day 0, SRD-13A cells were set up at 3.5×10^5 cells per 60 mm dish in medium C. On day 2, cells were transfected in 3 ml of medium A containing 5% FCS with the following plasmids: 2µg of pTK-HSV-SREBP-2, 0.5µg of pCMV-Scap, the indicated amount of wild-type pCMV-Insig-1-Myc (wt) (lanes 3 and 4), the D205E (lanes 5-8) or the D205R (lanes 9-12). The total DNA in each dish was adjusted to 3µg dish by addition of pcDNA3 mock vector. On day 3, cells were switched to medium B containing 1% HPCD and incubated for 1 hr at 37°C. Cells were then washed twice with PBS and switched to medium B in the absence or presence of 1µg/ml 25-HC plus 10µg/ml of cholesterol (sterols). After incubation for 5 hr, cells were harvested, and whole cell lysates were subjected to SDS-PAGE and immunoblot analysis with monoclonal IgG-9E10 (against Insig-1), polyclonal IgG-R139 (against Scap), and anti-HSV tag antibody (against SREBP-2). P and N denote precursor and nuclear forms of SREBP-2, respectively. Filters were exposed to film for 1-60s.

CHAPTER 3 STEROL-MEDIATED UBIQUITINATION AND DEGRADATION OF INSIG-1

Result

Insig-1 protein is stabilized by sterols

Figure 3-1 shows a pulse-chase experiment demonstrating that Insig-1 is rapidly degraded in sterol-depleted cells and that this degradation is blocked by sterols in the form of 25-HC. Wild-type CHO cells were depleted of sterols by prior inhibition with medium containing lipoprotein-deficient serum (LPDS) plus the cholesterol synthesis inhibitor compactin (an inhibitor of 3-hydroxy-3-methylglutaryl coenzyme A reductase [HMG CoA reductase]), and a low concentration of mevalonate (50 μM) to maintain nonsterol products for viability (Goldstein and Brown, 1990). After overnight incubation, cells were pulsed labeled for 1 hr with a mixture of ^{35}S-labeled methionine and cysteine, then washed and switched to isotope-free chasing medium in the absence or presence of 1 μg/ml of 25-HC for the indicated time. Insig-1 was isolated by immunoprecipitation, subjected to SDS-PAGE, and the ^{35}S-labeled protein was visualized in a phosphorimager. In the absence of any chase, hamster Insig-1 gives two bands on SDS-PAGE (Figure 3-1A, 0 time point) owing to the use of alternative translation initiation sites (Yang et al., 2002). The amount of ^{35}S-labeled Insig-1 rapidly decreased during the 2 hr chase period when cells were deplete of sterols, but remained stable once 25-HC was added. Radiometric quantitation demonstrated that the turnover rate of Insig-1 was clearly sterol regulated. In the absence of sterols, the calculated half-life of Insig-1 was around 20 min.

However addition of 25-HC prevented this degradation, and the half-life of the ^{35}S-labeled Insig-1 was extended by up to 2 hours (Figure 3-1B).

To study Insig-1 degradation without radioisotopes, I used SDS-PAGE and immunoblotting to follow the disappearance of total Insig-1 after protein synthesis was blocked by cycloheximide (CHX) (Figure 3-2). In the absence of sterols, endogenous Insig-1 disappeared within 30 min from wild-type CHO cells after CHX addition (Figure 3-2A, lanes 1-5). This rapid degradation was blocked by 25-HC (lanes 6-10). Since Insig-1 is known to be a direct downstream target of nuclear SREBPs, its protein level is subjected to transcriptional regulation according to the cellular cholesterol content. To focus on the study of post-translational modification of Insig-1, I generated a stable cell line expressing human Insig-1 under control of the constitutive thymidine kinase (TK) promoter in the Insig-1 deficient cells (SRD-14 cells) (Sever et al., 2004). Similar results were obtained when Myc epitope-tagged Insig-1 degradation was assessed after CHX treatment (Figure 3-2B).

Insig-1 degradation is mediated by proteasomes

In experiment shown in Figure 3-3, protein levels of Insig-1 were examined in cells with or without treatment of proteasome inhibitors. In the absence of inhibitors, the steady state level of Insig-1 was greatly increased after 5hr incubation with sterols (lanes 1 and 2). Addition of various proteasome inhibitors all raised Inisg-1 protein levels in cells depleted of sterols (lanes 3-8), demonstrating the rapid degradation of Insig-1 in sterol-depleted cells is mediated by proteasomes.

Sterol stabilization of Insig-1 requires Scap

The observation that 25-HC can greatly affect Insig-1 protein stability, coupled with previous results that Insig-1 forms complexes with both Scap and HMG CoA reductase in the presence of sterols lead us to test whether both proteins are involved in sterol dependent stabilization of Insig-1 (Yang et al., 2002; Sever et al., 2003). For this purpose, two mutant CHO cells defective in either protein were chosen. In UT-2 mutant cells that are defective in HMG CoA reductase (Mosley et al., 1983), endogenous Insig-1 preserved the sterol dependent turnover as observed in wild-type CHO-7 cells (Figure 3-4A), indicating HMG CoA reductase is not necessary for Insig-1 degradation. However, when SRD-13A cells, a line of mutant CHO-7 cells lacking functional Scap (Rawson et al., 1999) were transfected with pTK-Insig-1-Myc, the tagged protein was degraded rapidly after CHX treatment (Figure 3-4B, lanes 2-5), and there was no effect by 25-HC (lanes 6-9). In a similar experiment, when wild-type Scap was co-expressed, the degradation of Insig-1 was retarded even in the absence of 25-HC (Figure 3-5A, lanes 7-9), likely because the cells contained a low level of residual sterols. Degradation was further blocked when 25-HC was added (lanes 10-12). These data suggest that 25-HC alone could not block Insig-1 degradation and that sterol mediated stabilization of Insig-1 depends on the presence of Scap.

I next sought to determine the mechanism of the Scap requirement in Insig-1 stability. To further confirm that Scap binding mediates the stabilization of Insig-1, SRD-13A cells were transfected with a plasmid encoding Scap (Y298C), a mutant Scap that does not bind to Insigs (Adams et al., 2004). In SRD-13A cells producing Insig-1-Myc alone, the steady state levels of tagged Insig-1 were low in either the absence or presence

of 25-HC after 5 hr treatment (Figure 3-5B, lanes1 and 2). Co-expression of wild-type Scap stabilized Insig-1 in a sterol dependent fashion (lanes 3 and 4). Co-expression of mutant Scap (Y298C) did not stabilize Insig-1, even in the presence of 25-HC (lanes 5 and 6). Immunoblotting with an antibody against Scap confirmed that equal amounts of wild-type and Y298C were expressed (Figure 3-5B, bottom panel, lanes 3-6). When the cells were treated with MG-132, an inhibitor of the proteasome, the amount of Insig-1 became visible even in the absence of Scap (lane 7) and in cells expressing Scap (Y298C) (lane 11), and there was no further effect of 25-HC (lanes 8, 10, and 12).

Studies in Chapter 2 reported the D205A mutation in Insig-1 that abolishes the Insig-1/Scap complex formation. The experiment in Figure 3-6C was designed to test whether Scap was able to stabilize the D205A mutant in the presence of sterols. Consistent with earlier data, in SRD-13A cells producing Insig-1-Myc alone, Insig-1 levels were not detectable either in the absence or presence of 25-HC (Figure 3-6C, lanes 2 and 3). Addition of MG-132 stabilized Insig-1 by blocking the proteasomal degradation (lane 4). Similar results were observed when mutant Insig-1 (D205A) was overexpressed (lanes 5-7). Co-expression of Scap stabilized wild-type Insig-1 in the presence of sterols (lanes 8 and 9) as expected. However, it had no effect on the D205A mutant (lanes 10 and 11). Immunoblotting with an antibody against Scap confirmed that equal amounts of protein were expressed (bottom panel, lanes 8-11). These data further confirmed that full stabilization of Insig-1 requires the presence of sterols and a Scap that is capable of forming a functional ternary complex.

Ubiquitination precedes Insig-1 degradation

Most if not all proteins that undergo proteasomal degradation requires prior ubiquitination modification (Hershko and Ciechanover, 1998). To demonstrate ubiquitination of Insig-1, Scap deficient SRD-13A cells were transfected with a plasmid encoding Insig-1 and a plasmid encoding ubiquitin that contains an HA epitope tag. The cells were incubated in sterol-depleting medium, after which some of the dishes received 25-HC. For 2 hr prior to harvest, the cells were incubated with MG-132 to block the degradation of ubiquitinated Insig-1. Insig-1 was immunoprecipitated from detergent-solubilized lysates, and the precipitates were subjected to SDS-PAGE and blotted with an antibody to the HA tag on ubiquitin. In control cells not expressing T7-tagged Insig-1, no ubiquitin was seen in the Insig-1 immunoprecipitates (Figure 3-6A, lane 1). In cells expressing the tagged Insig-1, the anti-ubiquitin blot of the Insig-1 immunoprecipitate exhibited the typical smear seen with polyubiquitinated proteins (lane 2). The most rapidly migrating bands consisted of a doublet that migrated at the same position as authentic Insig-1. Since they were visualized with the anti-HA antibody, these bands likely represented Insig-1 that contained a minimal number of ubiquitins. In the absence of Scap, the addition of 25-HC did not affect Insig-1 ubiquitination (lane 3). Co-expression of Scap did not affect Insig-1 ubiquitination in the absence of sterols (lane 4), but it permitted 25-HC to block this ubiquitination (lane 5). Thus explains the mechanism that Scap stabilizes Insig-1 by inhibiting its ubiquitination. Although ubiquitinated Insig-1 was clearly seen when blotted with the antibody against the HA tag on ubiquitin, a higher-molecular-weight smear was not observed (data not shown) when Insig-1 was blotted with an antibody against the T7 epitope tag (IB: Insig-1 in Figure 3-6A). This is the usual finding in studies of protein ubiquitination in intact cells, and it is believed to

reflect the activity of de-ubiquiting enzymes that remove the ubiquitin when cell extracts are made. The amount of residual ubiquitinated Insig-1 is sufficient for visualization when blotted for ubiquitin but not when blotted for Insig-1.

Ubiquitination generally occurs on specific lysine residues oriented toward the cytoplasm. Insig-1 is predicted to contain four such residues at positions 33, 156, 158, and 273 (Feramisco et al., 2004). In preliminary mutagenesis experiments, it has been known that the lysines at positions 33 and 273 could be changed to arginines without affecting ubiquitination and degradation (data not shown). However, the closely spaced lysines at residues 156 and 158 were crucial. Figure 3-6B shows that wild-type Insig-1 was ubiquitinated as determined by immunoprecipitation of Insig-1 followed by blotting with anti-HA ubiquitin (lane 4). No ubiquitination was demonstrated when I expressed a plasmid encoding a mutant Insig-1 with arginines substituted for lysines at positions 156 and 158 (lane 5). The bottom autoradiogram of Figure 3-6B shows that equal amounts of wild-type and mutant Insigs were precipitated with the antibody against the T7 epitope on the Insigs. Mutant Insig-1 with only a single lysine mutation (K156R or K158R) was degraded as rapidly as wild-type Insig-1, suggesting that ubiquitination on either lysine is sufficient for proteasomal degradation (data not shown).

Ubiquitination of Insig-1 is not required for its dissociation from Scap

If ubiquitination is required for rapid degradation of Insig-1, then the K156R/K158R mutant should not be degraded, and it should not require Scap and 25-HC for stabilization. To test this hypothesis, SRD-14 cells, a line of mutant CHO cells that does not express Insig-1 was chosen (Sever et al., 2004). SRD-14 cells were stably transfected

with plasmids encoding wild-type Insig-1 or the K156R/K158R mutant under control of the thymidine kinase (TK) promoter. Stable lines expressing wild-type and mutant Insig-1 were prepared. In the absence of sterols, immunoblottable wild-type Insig-1 protein became undetectable within 60 min after CHX addition (Figure 3-6C, lanes 1-5), whereas no such disappearance was seen with the K156R/K158R Insig-1 mutant (lanes 11-15).

The question immediately arises as to whether ubiquitination and degradation of Insig-1 are essential to release the Scap/SREBP complex, or whether the complex can be released upon sterol deprivation even when ubiquitination and degradation do not occur. To answer this question, I studied the SRD-14 cells that were stably transfected with the cDNAs encoding either wild-type Insig-1 or the K156R/K158R mutant. Two types of sterol depletion methods were used for testing the SREBP response: 1) rapid sterol depletion by incubating the cells in hydroxypropyl-β-cyclodextrin (HPCD) (Figure 3-7); and 2) gradual sterol depletion by incubating the cells in serum from which the cholesterol-carrying lipoproteins had been removed (LPDS) (Figure 3-8). Prior to the start of both experiments, the cells were incubated with 25-HC to form the stable Insig-1/Scap/SREBP complex. The amount of Insig-1 and the amount of Scap that co-immunoprecipitated with Insig-1 were measured. The amount of nuclear SREBP-2 was also measured as the functional indicator of the complex status. In the rapid sterol-depletion experiment, the cells were treated with HPCD to remove cholesterol to extreme conditions (Figure 3-7). In cells expressing wild-type Insig-1, the amount of Insig-1 declined markedly within 1 hr (lane 1). At this point Scap no longer co-immunoprecipitated with Insig-1, and nuclear SREBP-2 was clearly visible. In cells expressing the K156R/K158R mutant, the amount of the Insig-1 protein remained high

throughout the experiment (lanes 6-10). Nevertheless, within 1 hr Scap no longer immunoprecipitated with Insig-1, and nuclear SREBP-2 was already being generated (lane 8).

Failure to ubiquitinate Insig-1 causes a delay in SREBP processing

To test the role of ubiquitination under more mild and physiological condition, a gradual sterol-depletion protocol using LPDS medium was used (Figure 3-8A). In cells expressing wild-type Insig-1 the amount of Insig-1 began to decline as early as 4 hr after initial sterol depletion. At this time point, there was a modest decline in the amount of Scap that co-immunoprecipitated with Insig-1 and a trace of nuclear SREBP-2 appeared (lane 2). By 8 hr, Insig-1 had declined further, Scap was no longer precipitated with Insig-1, and nuclear SREBP-2 was clearly detectable (lane 3). A delay in these processes was seen in the cells expressing the K156R/K158R mutant. At 8 hr, the amount of the mutant Insig-1 remained high, abundant Scap continued to co-immunoprecipitate with the Insig-1, and nuclear SREBP-2 was still not visible (lane 8). By 24hr, the mutant Insig-1 had declined, the amount of Scap in the immunoprecipitate fell, and nuclear SREBP-2 was clearly visible (lane 10). These data suggest that under conditions of gradual sterol depletion the failure to ubiquitinate Insig-1 caused a delay in release of the Scap/SREBP-2 complex, but it does not abolish it.

Figure 3-8B shows that the Insig-1 stability has a physiological influence on cell growth. When cultured in medium with low cholesterol-carrying lipoprotein (LPDS), cells expressing wild-type or the K156R/K158 mutant Insig-1 exhibit similar growth rate and reach confluence after 10 days. However, when cells were first incubated with 25-

HC to form the stable Insig-1/Scap/SREBP complex before switched back to regular LPDS medium, only wild-type Insig-1 expressing cells could survive. Addition of cholesterol to the medium after incubation of cells with 25-HC could rescue the growth defect in the mutant cells, indicating that these cells fail to proliferate as a result of cholesterol depletion.

Cholesterol and new Insig-1 converge on Scap to suppress SREBP cleavage

The data of Figure 3-7 indicate that upon severe sterol depletion the Scap/SREBP complex can dissociate from Insig-1 even when Insig-1 is not ubiquitinated or degraded. Thus, ubiquitination of Insig-1 is not required in order for Insig-1 to release Scap. What, then, is the role of ubiquitination and degradation? I hypothesized that this degradation is necessary in order to establish a condition in which SREBP processing can only be terminated when SREBPs have entered the nucleus, activated the *Insig-1* gene, and restored the level of Insig-1 protein.

To test this hypothesis, I performed sterol depletion experiments in wild-type cells that express Insig-1 from its natural promoter (Figure 3-9 and 3-10). In Figures 3-9A and 3-9B, wild-type CHO-7 cells were preincubated with 25-HC and then treated for 15 min with cyclodextrin to deplete sterols, followed by incubation in medium with LPDS. At zero time, Insig-1 was present, and there was no detectable nuclear SREBP-2 (Figure 3-9A). Insig-1 protein was observed despite a relatively low level of Insig-1 mRNA as measured by quantitative real-time PCR (see bar graph in Figure 3-9B), presumably because Insig-1 was protected from degradation by formation of the sterol-dependent Scap/Insig-1 complex. Within 0.75 hr of sterol depletion, most of the Insig-1 had been

degraded, nuclear SREBP-2 became visible, and the amount of Insig-1 mRNA had risen by 3-fold owing to transcriptional stimulation by nuclear SREBPs. The amount of Insig-1 protein began to increase as the level of Insig-1 mRNA rose. At 1.5 hr, FCS was added to the culture medium. FCS contains LDL, which supplies cholesterol to cells via the LDL receptor (Goldstein et al., 1983). At 5.5 hr, the amount of nuclear SREBP-2 began to decline, presumably owing to the formation of the cholesterol/Scap/Insig-1 complex. In response to the decline in nuclear SREBPs, the amount of Insig-1 mRNA declined but the amount of Insig-1 protein remained high, owing to its complex with Scap.

The data of Figures 3-9A and 3-9B, together with previous data in this paper, indicate that, upon acute sterol deprivation, the increase in nuclear SREBPs stimulates the uptake and synthesis of cholesterol as well as the synthesis of new Insig-1 molecules. The convergence of cholesterol and Insig-1 traps the Scap/SREBP complex in the ER, leading to a decline in nuclear SREBPs and Insig-1 mRNA, but a persistence of Insig-1 protein, owing to the stability of its complex with Scap. To confirm that cholesterol uptake is required for this convergent effect, I repeated the sterol-depletion experiment, but this time I incubated the cells in lipoprotein-deficient serum (LPDS) instead of FCS. In contrast to FCS, LPDS is devoid of LDL, and it cannot supply cholesterol to the cells. The results are shown in Figure 3-10. When cells were depleted of sterols and then placed in FCS, Insig-1 protein initially declined and nuclear SREBP-2 increased (Figure 3-10A). Thereafter, the reciprocal changes occurred, i.e. Insig-1 protein rose and nuclear SREBP-2 declined. These results duplicate the findings of Figure 3-9A. When the sterol-depleted cells were incubated in LPDS, the initial response was the same, i.e., Insig-1 fell and nuclear SREBP-2 increased (Figure 3-10B). However, in the absence of LDL-cholesterol,

the subsequent rise in Insig-1 was delayed and there was no fall in nuclear SREBP-2. This result indicates that the cells require the convergence of cholesterol and Insig-1 in order to block SREBP processing. Endogenous cholesterol synthesis is not sufficient to satisfy the cholesterol requirement over the short term of this experiment, and therefore LDL-derived cholesterol is essential.

Figure 3-11 shows the opposite result to that in Figures 3-9 and 3-10 – namely, the response of sterol-depleted CHO cells to the addition of 25-HC. In this experiment, the cells were preincubated in LPDS to deplete sterols, and then 25-HC was added. At zero time, the sterol-deprived cells contained a relatively small amount of Insig-1 protein, no Scap was co-immunoprecipitated with Insig-1, and the content of nuclear SREBP-2 was high (Figure 3-11A). The amount of Insig-1 mRNA was also high, presumably owing to the high level of nuclear SREBPs (Figure 3-11B). Within 0.5 hr after adding 25-HC, the amount of Insig-1 had risen detectably, Scap became visible in the Insig-1 immunoprecipitate, and the amount of nuclear SREBP-2 had begun to decline. Insig-1 mRNA remained high. By 1 hr, Insig-1 protein reached a peak, as did the amount of Scap in the Insig-1 immunoprecipitate. Nuclear SREBP-2 was reduced by more than 90%. The fall in Insig-1 mRNA levels lagged behind the drop in nuclear SREBP-2, apparently owing to the half-life of the mRNA, but by 3 hr the Insig-1 mRNA had declined by more than 90%. Despite this decline in mRNA, the Insig-1 protein was accumulating, presumably owing to its stabilization in the Scap/Insig-1 complex. At the conclusion of the experiment (4 hr), the level of Insig-1 protein was the same as it was at zero time, even though Insig-1 mRNA had declined by 95%.

Discussion

The data presented in this Chapter revealed the physiological role of the regulated degradation of Insig-1 in the feedback control of cholesterol synthesis and uptake. When cellular cholesterol levels are low, Scap dissociates from Insig-1, which is then ubiquitinated on lysines 156 and 158 and degraded in proteasomes. This rapid degradation of Insig-1 helps to free the Scap/SREBP complex so that the SREBP can be processed to the nuclear form to activate the target genes, thus replete the cholesterol levels within the cell. Simultaneously, the newly synthesized Insig-1 proteins are also inserted to the ER membranes as a result of nSREBPs activation. When sterols accumulate to a certain point, the new Insig-1 and cholesterol converge on Scap. This binding prevents Insig-1 from degradation and allows the Insig-1/Scap/SREBP to be retained in the ER, ready for liberation when the cell is again sterol deprived.

This process is proposed as a "convergent feedback inhibition" because it requires two coordinated conditions: 1) Insig-1 must be destroyed after sterol depletion, and 2) SREBPs must activate the synthesis of replacement Insig-1 molecules as well as the genes supplying cholesterol. Destruction of Insig-1 creates a requirement for newly synthesized Insig-1, which cannot occur unless sufficient SREBP molecules have entered the nucleus. Thus, sterol synthesis will not be suppressed unless SREBPs have acted on two processes: 1) cholesterol supply through de novo synthesis and uptake via LDL receptors, and 2) *Insig-1* gene transcription.

The significance of the two components of the Insig-1 control mechanism is underscored by a comparison with Insig-2. In contrast to Insig-1, Insig-2 is neither rapidly degraded nor is it a transcriptional target of SREBPs. The fact that Insig-1

uniquely possesses both attributes emphasizes the necessity for rapid, sterol-regulated degradation coupled to transcriptional activation in order for the convergent control mechanism to operate.

If Insig-2 does not participate in convergent feedback, what is its role? Studies of mutant CHO cells suggest that Insig-2 functions in long-term control of SREBP processing. Thus, SRD-14 cells lack Insig-1 as a result of loss-of-function of both alleles of the *Insig-1* gene, but they express normal amounts of Insig-2 protein (Sever et al., 2004). In SRD-14 cells, 25-HC fails to block SREBP processing acutely within 5 hr after exposure. However, after 14 hr SREBP-2 processing is blocked. Thus, at normal levels of expression, Insig-2 cannot replace Insig-1 in achieving short-term control of SREBP processing. The long-term function of Insig-2 may help to smooth out oscillations in SREBP processing that might otherwise occur as Insig-1 levels rise and fall through the convergent feedback mechanism. This would be analogous to the roles of the several isoforms of IκB, a family of proteins that play roles in the NF-κB pathway (Hoffmann et al., 2002) that are similar to those of Insigs in the SREBP pathway. Insig-2 may play a more important role than Insig-1 in the liver, where higher amounts of Insig-2 are produced through the action of a liver-specific promoter that is down-regulated by insulin (Yabe et al., 2003).

Material and Methods

Materials

I obtained MG-132, lactacystin, epoxomicin and nonidet P-40 from Cal Biochem; cycloheximide from Sigma; all sterols from Steraloids, Inc.; hydroxypropyl-β-cyclodextrin from Cyclodextrin Technologies Development, Inc.; and fos-choline 13 from Anatrace, Inc. Lipoprotein-deficient newborn calf serum (d > 1.215 g/ml) was prepared by ultracentrifugation (Goldstein, J. L., Basu, S. K., and Brown, M. S. (1983) *Methods Enzymol.*). Solutions of sodium compactin, sodium mevalonate, and sodium oleate were prepared as described (Kita et al., 1980; Hannah et al., 2001)

Antibodies

I obtained horseradish peroxidase-conjugated, donkey anti-mouse, and anti-rabbit IgGs (affinity-purified) from Jackson Immunoresearch Laboratories; polyclonal anti-HA IgG from Santa Cruz Biotechnology, Inc.; polyclonal anti-Myc and anti-T7 IgGs from Bethyl Laboratories; and cells producing IgG-9E10, a mouse monoclonal antibody against Myc tag, from American Type Culture Collection. IgG-7D4, a mouse monoclonal antibody against hamster SREBP-2 (Sakai, J.1996 Cell); IgG-9D5, a mouse monoclonal antibody against hamster Scap (Sakai et al., 1997); and IgG-R139, a rabbit polyclonal antibody against hamster SCAP (Sakai, J. 1997 JBC), were previously described in the indicated references; Polyclonal antiserum against hamster Insig-1 was produced by immunizing rabbits with a mixture of two peptides from hamster Insig-1 protein sequence (amino acids 14-23 and amino acids 32-50).

Plasmid Constructs

The following recombinant plasmids have been described: pEF1a-HA-ubiquitin (provided by Dr. Zhijian Chen, University of Texas Southwestern Medical Center), encoding amino acids 1-76 of human ubiquitin preceded by an epitope tag derived from the influenza hemagglutinin (HA) protein (YPYDVPDY) under the control of the EF1a promoter (Kanayama et al., 2004); pCMV-Insig-1-T7, encoding human Insig-1 followed by three copies of a T7 epitope tag (MASMTGGQQMG) under control of the cytomegalovirus (CMV) promoter (Song et al., 2005); pCMV-Scap, encoding wild-type hamster Scap under control of CMV promoter (Sakai et al., 1997); and pTK-Scap and pTK-Scap(Y298C), encoding wild-type and mutant hamster Scap, respectively, under control of the thymidine kinase (TK) promoter (Nohturfft et al., 1998). pTK-Insig-1-Myc encoding wild-type human Insig-1 followed by six tandem copies of a c-Myc epitope tag(EQKLISEEDL) under control of the TK promoter was generated by the following method. First, pTK-HSV-SREBP-2(Hua et al., 1996) was digested with NheI and XbaI to remove HSV-SREBP-2, and the six kb backbone fragment was isolated. Second, the coding region of human Insig-1 (amino acids 1-277), with six tandem copies of a c-Myc epitope tag at the NH2-terminus was amplified by PCR using pCMV-Insig-1-Myc(Yang et al., 2002) as a template. Forward and reverse primers used for PCR were as follows: 5’-CTACGATCGCTAGCATGCCCAGATTGCACGACCACTTCTGGAGCTGCTC-3’ and5’-TAGGGCCCTCTAGATCAACTATTAAGATCCTCCTCGGATATTAACTTCTGCTCAC-3’ (underlines denotes NheI and XbaI sites). The PCR product containing human Insig-1 followed by six Myc tags was digested with NheI and XbaI and ligated into the pTK vector from pTK-HSV-SREBP-2 between the NheI and XbaI sites. A plasmid with

the correct orientation was selected. pTK-Insig-1(K156R/K158R)-Myc and pCMV-Insig-1(K156R/K158R)-T7 were generated by site-directed mutagenesis using the QuikChange site-directed mutagenesis kit (Stratagene). The coding regions of all plasmids were sequenced before use.

Tissue Culture Media

Medium A contains a 1:1 mixture of Ham's F-12 medium and Dulbecco's modified Eagle's medium supplemented with 100 units/ml penicillin and 100 μg/ml streptomycin sulfate. Medium B contains medium A supplemented with 5% (v/v) newborn calf lipoprotein-deficient serum, 50 μM sodium compactin and 50μM sodium mevalonate. Medium C contains medium A supplemented with 5% (v/v) fetal calf serum, 5 μg/ml cholesterol, 1 mM sodium mevalonate, and 20 μM sodium oleate. Medium D contains methionine- and cysteine-free RPMI 1640 medium supplemented with 5% (v/v) newborn calf lipoprotein-deficient serum, 50 μM sodium compactin and 50μM sodium mevalonate. Medium E contains medium A supplemented with 5% FCS and 0.2 mM mevalonate.

Cell Culture

Cells were maintained in monolayer culture at 37 °C in 8–9% CO_2. CHO-7 cells are a clone of CHO-K1 cells selected for growth in lipoprotein-deficient serum (Metherall et al., 1989). UT-2 cells (HMG CoA reductase$^{-/-}$) are mutant cells derived from CHO-K1 cells (Mosley et al., 1983). SRD-13A cells (Scap$^{-/-}$) (Rawson et al., 1999) and SRD-14 cells (Insig-1 $^{-/-}$) (Sever et al., 2004) are mutant cells derived from CHO-7 cells. SRD-14/pTK-Insig-1-Myc cells are a clone of SRD-14 cells stably transfected with pTK-Insig-

1-Myc (see below). SRD-14/pTK-Insig-1(K156R/K158R)-Myc cells are a clone of SRD-14 cells stably transfected with pTK-Insig-1(K156R/K158R)-Myc (see below).

Stock cultures of CHO-7 cells were maintained in medium A supplemented with 5% (v/v) newborn calf lipoprotein-deficient serum. UT-2 cells were maintained in medium E. SRD-13A cells were maintained in medium C. SRD-14/pTK-Insig-1-Myc cells and SRD-14/pTK-Insig-1(K156R/K158R)-Myc cells were maintained in medium A supplemented with 5% (v/v) newborn calf lipoprotein-deficient serum and 500 μg/ml G418.

Transient Transfection of Cells

CHO-7 and SRD-13A cells were transiently transfected with FuGENE 6 reagent (Roche Applied Science) according to the manufacturer's protocol. The total amount of DNA in each transfection was adjusted to 3 μg per dish by addition of pcDNA3 mock vector. Conditions of incubation after transfection are described in the Figure legends. At the end of the incubation, duplicate dishes of cells for each variable were harvested and pooled for analysis.

Stable Transfection of Cells

SRD-14/pTK-Insig-1-Myc and SRD-14/pTK-Insig-1(K156R/K158R)-Myc cells, derivatives of SRD-14 cells were generated as follows. On day 0, SRD-14 cells were set up at 5×10^5 cells per 100-mm dish in medium A with 5% (v/v) newborn calf lipoprotein-deficient serum. On day 1, the cells were transfected with 1 μg of pTK-Insig-1-Myc or pTK-Insig-1(K156R/K158R)-Myc using the FuGENE 6 transfection reagent as described

above. On day 2, cells were switched to medium A supplemented with 5% (v/v) newborn calf lipoprotein-deficient serum and 700 μg/ml G418. Fresh medium was added every 2-3 days until colonies formed after about 2 weeks. Individual colonies were isolated with cloning cylinders, and Insig-1 expression was assessed by immunoblot analysis with anti-Myc. Cells were chosen based on their transgene expression such that Insig-1 expression level in SRD-14/pTK-Insig-1-Myc cells is equal to that in SRD-14/pTK-Insig-1(K156R/K158R)-Myc cells in the presence of 1μg/ml of 25-HC. Cells from a single colony were cloned by limiting dilution and maintained in medium A containing 5% (v/v) newborn calf lipoprotein-deficient serum and 500 μg/ml G418.

Immunoblot Analysis

To prepare a whole-cell lysate fraction, cell pellets from duplicate dishes were resuspended in 0.2 ml of buffer (50 mM HEPES-KOH [pH 7.6], 100 mM NaCl, 1.5 mM $MgCl_2$, 1% NP-40, and protease inhibitor cocktail consisting of 10 μg/ml leupeptin, 5 μg/ml pepstatin A, 25 μg/ml ALLN, and 2 μg/ml aprotinin), rotated at 4°C for 30 min, and centrifuged at 20,000g for 20 min at 4°C. The supernatant from this spin was mixed with 5X SDS loading buffer(150 mM Tris-Cl at ph 6.8, 15% SDS, 25% (v/v) glycerol, 0.02% (w/v) bromophenol blue, and 12.5% (v/v) 2-mercaptoethanol).

All fractions were subjected to SDS-PAGE and immunoblot analysis as previously described (Sakai, J. 1996 cell). The primary antibodies used for immunoblotting are given in the Figure legends. Secondary antibodies were horseradish peroxidase-conjugated donkey anti-mouse and anti-rabbit IgGs (1: 5000 dilution). Bound secondary antibodies were visualized by chemiluminescence using the SuperSignal

substrate system (Pierce) according to the manufacturer's instructions. Filters were exposed to Kodak X-Omat Blue XB-1 films at room temperature for indicated time.

Immunoprecipitation

The pooled cell pellets from duplicate dishes of cells were resuspended in 0.5 ml of buffer A (50 mM HEPES-KOH [pH 7.6], 100 mM NaCl, 1.5 mM $MgCl_2$, 0.1% NP-40, and protease inhibitors (see above)). Cell lysates were prepared and immunoprecipitation was performed as described (Sakai, J. 1997 JBC) with the following modifications. Precleared lysates were rotated for 16 h at 4°C with 20 µg of either control nonimmune IgG, polyclonal antiserum against hamster Insig-1 (1:100 dilution), or polyclonal anti-Myc (40 µg/ml) together with 50 µl of protein A/G agarose beads (Santa Cruz Biotechnology). After centrifugation, the resulting supernatants were mixed with 5X SDS loading buffer. The pelleted beads were washed three times(20 min each at 4°C) with 1 ml of buffer A; resuspended in 100 µl of buffer containing 10 mM Tris-HCl [pH 6.8], 1% (w/v) SDS, 100 mM NaCl and protease inhibitors; and mixed with 5X SDS loading buffer. Supernatants and pellets were boiled for 5 min, and subjected to SDS/PAGE and immunoblot analysis.

Real-time PCR

The protocol was identical to that described by Liang *et al*. (Liang, G. 2002 JBC). Triplicate samples of first-strand cDNA were subjected to real-time PCR quantification using forward and reverse primers for the indicated mRNA with hamster actin as an

invariant control. Relative amounts of mRNAs were calculated using the comparative C_T method.

Pulse-Chase Analysis in CHO-7 Cells

CHO-7 cells were incubated in medium B as described above. Sixteen hours after incubation, cells were washed with phosphate-buffered saline and switched to methionine/cysteine-free medium D. After 1 h at 37 °C, the cells were pulse-labeled with 200 μCi/ml ^{35}S-Protein Labeling Mix (PerkinElmer Life Sciences) in 1.5 ml of medium D. After labeling for 1 h, the medium was removed, and the cells were washed twice with phosphate-buffered saline and chased for various times in medium B(containing 0.12mM unlabeled methionine and 0.4mM unlabeled cysteine) in the absence or presence of 1 μg/ml 25- hydroxycholesterol. Following the chase, the medium was removed, and the cells were washed three times with cold phosphate-buffered saline, lysed in 1 ml of buffer B (50 mM Tris-HCl at pH 7.2 and 0.15 M NaCl, 0.5% (v/v) Fos-Choline 13, and protease inhibitor cocktail). The lysate was clarified by centrifugation at 20,000*g* for 20 min at 4 °C. The supernatant was transferred to new tubes, and precleared by rotation for 16 h at 4 °C with 50 μl of protein A/G-agarose (Santa Cruz Biotechnology) and 20 μg/ml control nonimmune IgG. After centrifugation at 300*g* for 7 min at 4 °C, the supernatant was transferred to a fresh tube, and 10 μl of polyclonal antiserum against Insig-1(1:100 dilution) together with 50 μl of protein A/G-agarose beads were added and rotated for 2 hr at 4°C. The beads were collected by centrifugation, washed six times (30 min each) in 1 ml of buffer B, resuspended in 50 μl of 1x SDS loading buffer, and boiled for 5 min. After centrifugation at 16,000*g* for 5 min at room temperature, the supernatant was

transferred to a fresh tube, and aliquots of the immunoprecipitates were subjected to 12% SDS-PAGE. Radiolabeled proteins were transferred to Hybond C-Extra nitrocellulose filters. The filters were dried, exposed to an imaging plate at room temperature for 24 h, and scanned in a Molecular Dynamics Storm 820 phosphorimaging device.

Ubiquitination of Insig-1

Conditions of transfections and incubations are described in the figure legends. At the end of the incubation, cells were lysed in 0.1ml of buffer B supplemented with 10 mM *N*-ethylmaleimide, rotated at 4 °C for 1 hr, and centrifuged at 100,000 g for 15 min at 4 °C . The resulting supernatant was mixed with 0.3 ml of 8M urea in buffer B, rotated for 10 min at room temperature, diluted with buffer B to decrease the urea concentration to 2M, and subjected to immunoprecipitation (16 hrs at 4 °C) with 50 µl monoclonal anti-T7 IgG-coupled agarose beads (Novagen) directed against the epitope tag on Insig-1, followed by low-speed centrifugation. The resulting supernatants were mixed with 5X SDS loading buffer, and the pelleted beads were washed three times (20 min each) with buffer B and resuspended in 50 µl of 1XSDS loading buffer. The supernatant and pellet fractions were boiled for 5 min and subjected to SDS-PAGE and immunoblotting analysis against the HA tag on ubiquitin.

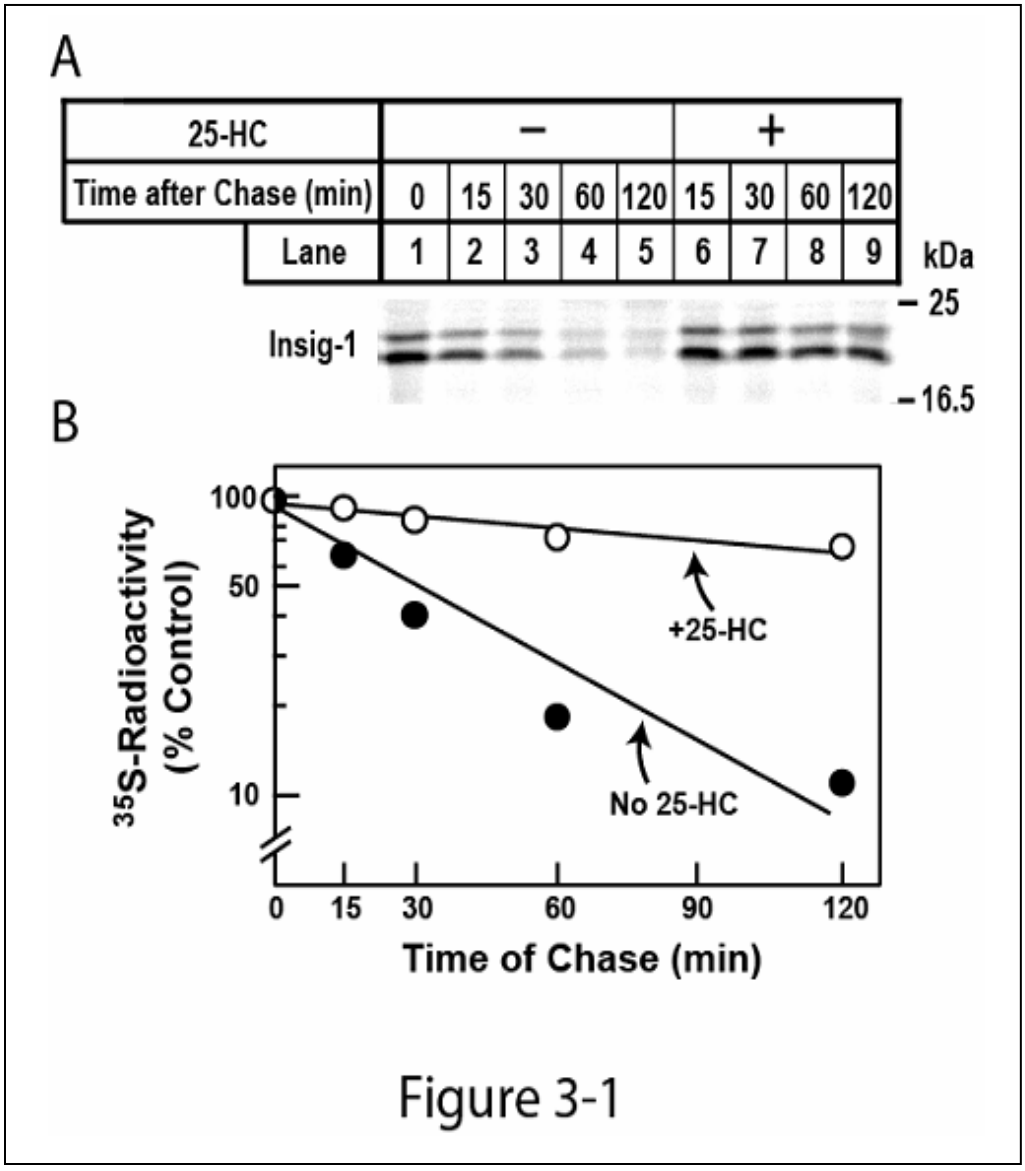
A
25-HC
−
+
Time after Chase (min)
0
15
30
60
120
15
30
60
120
Lane
1
2
3
4
5
6
7
8
9
kDa
25
Insig-1
16.5
B
100
50
10
35S-Radioactivity
(% Control)
+25-HC
No 25-HC
0
15
30
60
90
120
Time of Chase (min)

Figure 3-1

Figure 3-1 Sterol-regulated degradation of ^{35}S-labeled Insig-1 in hamster cells.

A) On day 0, CHO-7 cells were set up at 7.5×10^5 cells per 60 mm dish in medium A supplemented with 5% lipoprotein-deficient serum (LPDS). On day 1, cells were refed with sterol-depleting medium B. After 16 hr, cells were preincubated for 1 hr in methionine- and cysteine-free medium D, after which they were pulsed-labeled for 1hr with 200 μCi/ml ^{35}S-Protein Labeling Mix in medium D. Cells were then washed and incubated in medium B (containing unlabeled methionine and cysteine) in the absence (-) or presence (+) of 1 μg/ml 25-HC. Following the indicated incubation period, cells were harvested and lysed, and the whole-cell lysates were subjected to immunoprecipitation with polyclonal antiserum against Insig-1 (1:100 dilution). Aliquots of immunoprecipitates were subjected to 12% SDS-PAGE and transferred to nitrocellulose filters. Filters were exposed for 24 hr to an imaging plate at room temperature and scanned as described in Experimental Procedures.

B) Quantification of ^{35}S-radioactivity corresponding to Insig-1 in (A). The intensity of Insig-1 during the pulse (zero time value) was arbitrarily set at 100%.

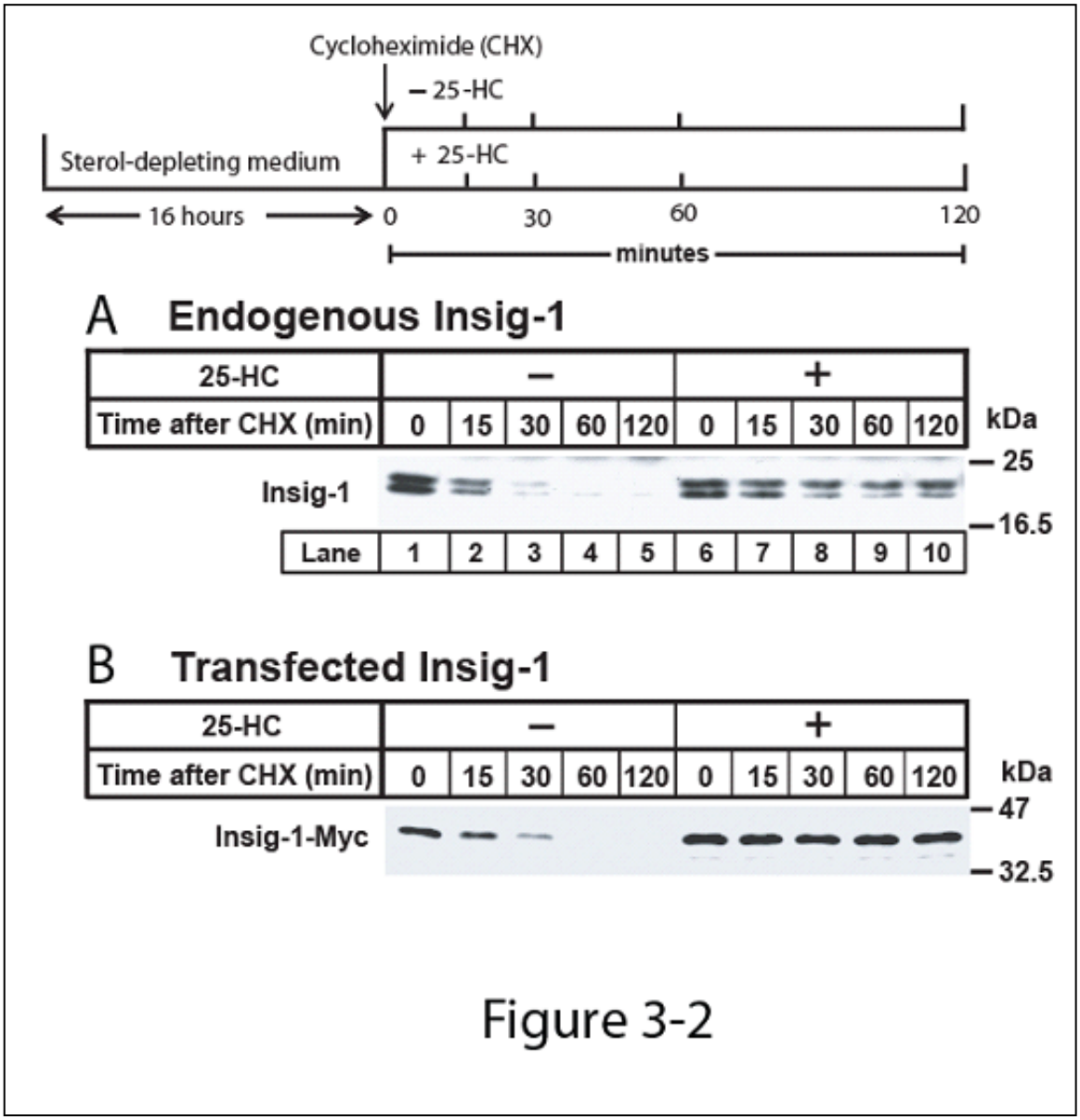
Cycloheximide (CHX)
– 25-HC
+ 25-HC
Sterol-depleting medium
16 hours
0
30
60
120
minutes
A Endogenous Insig-1
25-HC
–
+
Time after CHX (min)
0 15 30 60 120 0 15 30 60 120
kDa
Insig-1
25
16.5
Lane
1 2 3 4 5 6 7 8 9 10
B Transfected Insig-1
25-HC
–
+
Time after CHX (min)
0 15 30 60 120 0 15 30 60 120
kDa
Insig-1-Myc
47
32.5

Figure 3-2

Figure 3-2 Inhibition of degradation of endogenous and transfected Insig-1 by 25-hydroxycholesterol in hamster cells.

A) On day 0, CHO-7 cells were set up at 5×10^5 cells per 100 mm dish in medium A supplemented with 5% LPDS. On day 2, cells were refed with sterol-depleting medium B. After 16 hr (see schematic), cells were switched to fresh medium B containing 50 μM cycloheximide (CHX) in the absence (-) or presence (+) of 1 μg/ml of 25-HC. At the indicated time after CHX exposure, cells were harvested, and aliquots of whole-cell lysates were subjected to 10% SDS-PAGE and immunoblot analysis with a 1:1000 dilution of polyclonal antiserum against Insig-1.

B) On day 0, SRD-14/pTK-Insig-1-Myc cells were set up at 5×10^5 cells per 100 mm dish in medium A supplemented with 5% LPDS. On day 2, cells were refed with sterol-depleting medium B. After 16 hr (see schematic), cells were switched to fresh medium B containing 50 μM CHX in the absence (-) or presence (+) of 1 μg/ml of 25-HC. At the indicated time after CHX addition, cells were harvested and fractionated, and aliquots of whole-cell lysates were subjected to 10% SDS-PAGE and immunoblot analysis with 2μg/ml monoclonal anti-Myc IgG against Insig-1. In (A) and (B), filters were exposed to film for 30s.

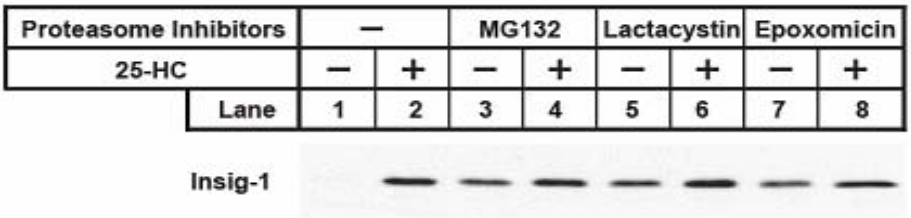
Proteasome Inhibitors
—
MG132
Lactacystin
Epoxomicin
25-HC
— + — + — + — +
Lane
1 2 3 4 5 6 7 8
Insig-1

Figure 3-3

Figure 3-3 Insig-1 degradation is mediated by proteasomes.

On day 0, SRD-14/pTK-Insig-1-Myc cells were set up at 7×10^5 cells per 60 mm dish in medium A supplemented with 5% LPDS. On day 1, cells were refed with sterol-depleting medium B. On day 2, cells were switched to fresh medium B containing 10μM of various proteasome inhibitors in the absence (-) or presence (+) of 1 μg/ml of 25-HC. After incubation for 5 hr, cells were harvested and fractionated, and aliquots of whole-cell lysates were subjected to 10% SDS-PAGE and immunoblot analysis with 5 μg/ml of monoclonal anti-Myc IgG (against Insig-1). Filter was exposed to film for 5s.

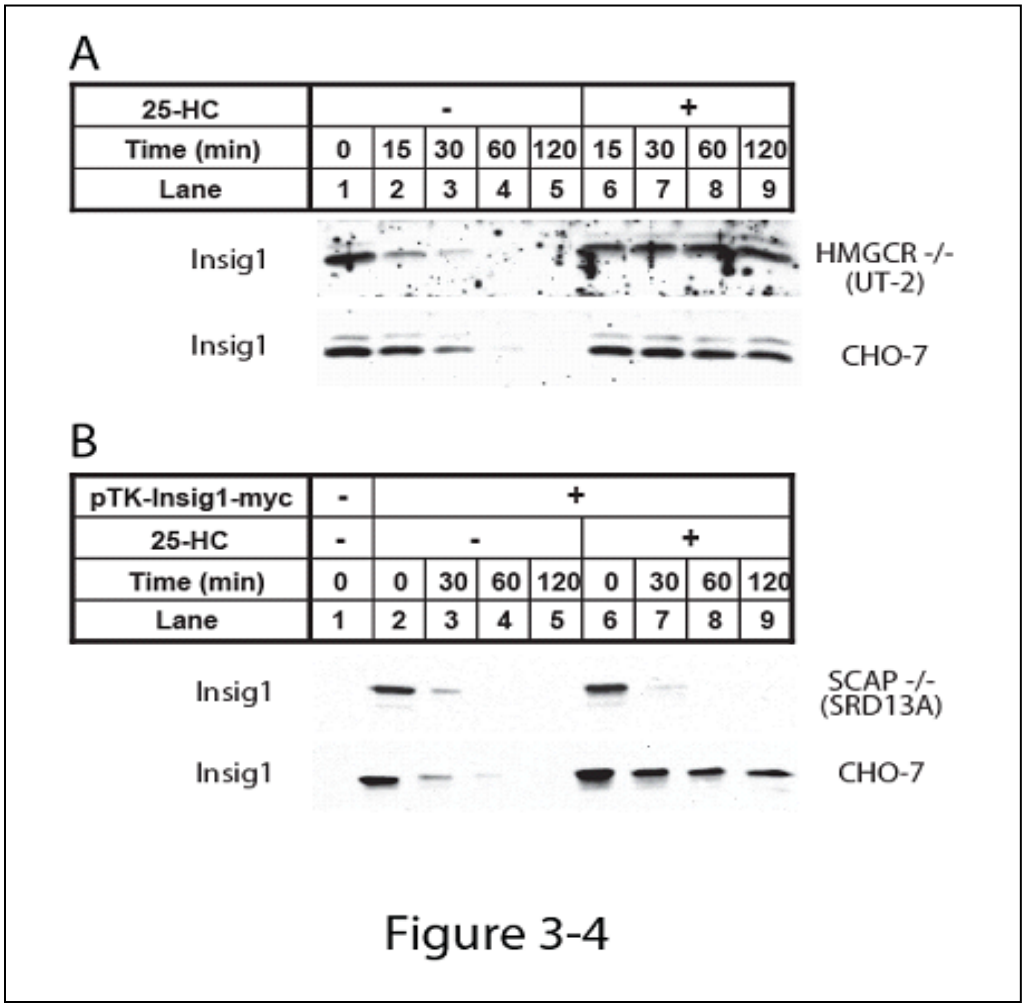
A
25-HC
-
+
Time (min)
0
15
30
60
120
15
30
60
120
Lane
1
2
3
4
5
6
7
8
9
Insig1
HMGCR -/-
(UT-2)
Insig1
CHO-7
B
pTK-Insig1-myc
-
+
25-HC
-
-
+
Time (min)
0
0
30
60
120
0
30
60
120
Lane
1
2
3
4
5
6
7
8
9
Insig1
SCAP -/-
(SRD13A)
Insig1
CHO-7

Figure 3-4

Figure3-4 Scap, but not HMG CoA reductase is required for sterol dependent stabilization of Insig-1.

A) On day 0, CHO-7 cells were set up at 5×10^5 cells per 100 mm dish in medium A supplemented with 5% LPDS. UT-2 cells were set up at 5×10^5 cells per 100 mm dish in medium E. On day 2, cells were refed with sterol-depleting medium B. After 16 hr, cells were switched to fresh medium B containing 50 μM cycloheximide (CHX) in the absence (-) or presence (+) of 1 μg/ml of 25-HC. At the indicated time after CHX exposure, cells were harvested, and aliquots of whole-cell lysates were subjected to 10% SDS-PAGE and immunoblot analysis with a 1:1000 dilution of polyclonal antiserum against Insig-1.

B) On day 0, SRD-13A cells were set up at 5×10^5 cells per 100 mm dish in medium C. CHO-7 cells were set up at 5×10^5 cells per 100 mm dish in medium A supplemented with 5% LPDS. On day 2, cells were transfected in 3 ml of medium A containing 5% FCS with 0.2 μg pTK-Insig-1-Myc. The total DNA in each dish was adjusted to 3μg/dish by addition of pcDNA3 mock vector. Six hours after transfection, cells were refed with sterol-depleting medium B. After 16 hr, cells were switched to fresh medium B containing 50 μM CHX in the absence (-) or presence (+) of 1 μg/ml of 25-HC. At the indicated time after CHX addition, cells were harvested and fractionated, and aliquots of whole-cell lysates were subjected to 10% SDS-PAGE and immunoblot analysis with 2μg/ml of monoclonal anti-Myc IgG against Insig-1. In (A) and (B), filters were exposed to film for 5-60s.

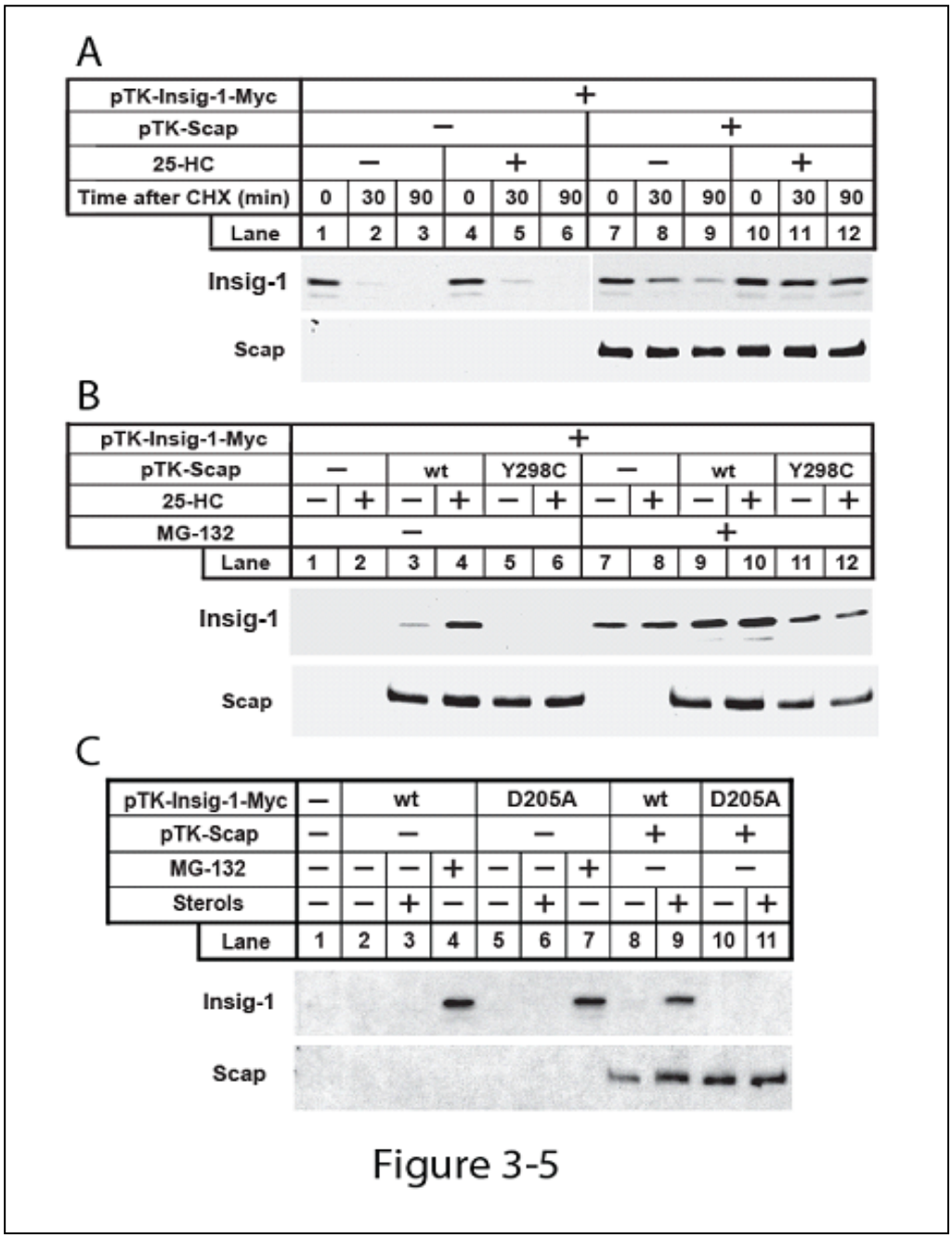
A
pTK-Insig-1-Myc
pTK-Scap
25-HC
Time after CHX (min)
Lane
Insig-1
Scap
B
pTK-Insig-1-Myc
pTK-Scap
25-HC
MG-132
Lane
Insig-1
Scap
C
pTK-Insig-1-Myc
pTK-Scap
MG-132
Sterols
Lane
Insig-1
Scap

Figure 3-5

Figure 3-5 Slowing of Insig-1 degradation requires sterol-dependent interaction with Scap.

On day 0, Scap-deficient SRD-13A cells were set up at 3.5×10^5 cells per 60 mm dish in medium C.

A) On day 2, cells were transfected in 3 ml of medium A containing 5% FCS with 1 μg pTK-Insig-1-Myc (lanes 1-12) with (lanes 7-12) or without (lanes 1-6) 1μg pTK-Scap as indicated. The total DNA in each dish was adjusted to 3μg by addition of pcDNA3 mock vector. Six hours after transfection, cells were refed with sterol-depleting medium B. After 16 hr, cells were switched to fresh medium B containing 50 μM CHX in the absence (-) or presence (+) of 1 μg/ml of 25-HC. At the indicated time after CHX treatment, cells were harvested and fractionated, and aliquots of whole-cell lysates were subjected to SDS-PAGE and immunoblot analysis with 5 μg/ml of monoclonal anti-Myc IgG (against Insig-1) and 5 μg/ml polyclonal IgG-R139 (against Scap). Filters were exposed to film for 30 s (lanes 1-6) and 5s (lanes 7-12) for Insig-1 and 1 min for Scap.

B) On day 2, cells were transfected in 3 ml of medium A containing 5% FCS with 0.2 μg pTK-Insig-1-Myc and 1 μg of either wild-type (wt) pTK-Scap or a mutant version (Y298C) as indicated. The total DNA was adjusted to 3 μg by addition of pcDNA3 mock vector. Six hours after transfection, cells were refed with sterol-depleting medium B. After 16 hr, cells were switched to fresh medium B containing 10 μM MG132 (lanes 7-12) in the absence (-) or presence (+) of 1 μg/ml of 25-HC. After incubation for 5 hr, cells were harvested and fractionated, and aliquots of whole-cell lysates were subjected to 8% or 10% SDS-PAGE and immunoblot analysis with 5 μg/ml of monoclonal anti-Myc IgG (against Insig-1) and 5 μg/ml polyclonal IgG-R139 (against Scap). Filters were exposed to film for 5 s (Insig-1) or 1 min (Scap).

C) On day 2, cells were transfected in 3 ml of medium A containing 5% FCS with the following plasmids: 1μg pTK-Scap, 0.2μg of wild-type pCMV-Insig1-Myc or the D205A. The total DNA in each lane was adjusted to 3μg/dish by addition of pcDNA3 mock vector. Six hours after transfection, cells were refed with sterol-depleting medium B. After 16 hr, cells were switched to fresh medium B containing 10μM MG-132 (lanes 4 and 7) in the absence (-) or presence (+) of 0.1 μg/ml of 25-HC. After incubation for 5 hr, cells were harvested, and whole cell lysates were subjected to SDS-PAGE and immunoblot analysis with IgG-9E10 (against Insig-1), IgG-R139 (against Scap). Filters were exposed to film for 10-60s.

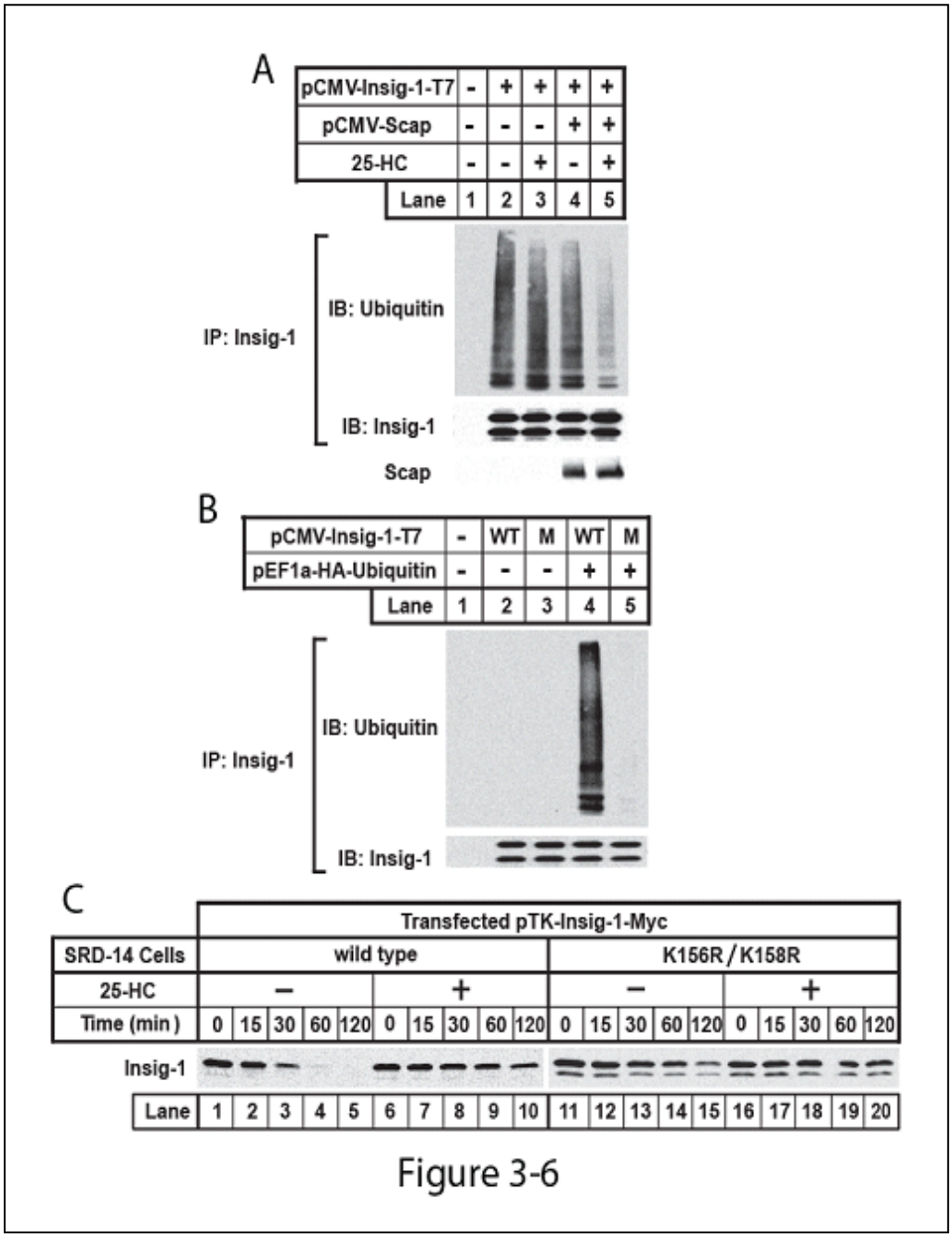
A
pCMV-Insig-1-T7 - + + + +
pCMV-Scap - - - + +
25-HC - - + - +
Lane 1 2 3 4 5
IP: Insig-1
IB: Ubiquitin
IB: Insig-1
Scap
B
pCMV-Insig-1-T7 - WT M WT M
pEF1a-HA-Ubiquitin - - - + +
Lane 1 2 3 4 5
IP: Insig-1
IB: Ubiquitin
IB: Insig-1
C
Transfected pTK-Insig-1-Myc
SRD-14 Cells
wild type
K156R / K158R
25-HC
–
+
Time (min) 0 15 30 60 120 0 15 30 60 120 0 15 30 60 120 0 15 30 60 120
Insig-1
Lane 1 2 3 4 5 6 7 8 9 10 11 12 13 14 15 16 17 18 19 20

Figure 3-6

Figure 3-6 Lysine 156 and lysine 158 are required for sterol-mediated ubiquitination and degradation of Insig-1 in hamster cells.

A) On day 0, Scap-deficient SRD-13A cells were set up at 3.5×10^5 cells per 60-mm dish in medium C. On day 2, cells were transfected in 3 ml of medium A containing 5% FCS with 0.2 μg of pEF1a-HA-ubiquitin, 0.2 μg pCMV-Insig-1-T7 and 1 μg of pCMV-Scap as indicated. The total DNA in each lane was adjusted to 3μg/dish by addition of pcDNA3 mock vector. Six hours after transfection, cells were refed with sterol-depleting medium B. After 16 hr, cells were switched to fresh medium B in the absence (-) or presence (+) of 1 μg/ml of 25-HC. After incubation for 3 hr, each dish received 10 μM MG-132. Following incubation at 37 °C for 2 hr, cells were harvested and subjected to immunoprecipitation with monoclonal anti-T7 IgG-coupled agarose beads. Aliquots of cell lysates and immunoprecipitates were subjected to SDS-PAGE (6% for ubiquitin blot, 8% for Scap, 10% for Insig-1) and immunoblot analysis with 1:1000 dilution of polyclonal anti-HA IgG (against ubiquitin), 1:15,000 dilution of polyclonal anti-T7 IgG (against Insig-1) and 5 μg/ml polyclonal IgG-R139 (against SCAP). Filters were exposed to film for 5s.

B) On day 0, SRD-13A cells were set up as in (A). On day 2, cells were transfected in 3 ml of medium A containing 5% FCS with 0.2 μg of pEF1a-HA-ubiquitin, 0.2 μg of with wild-type (wt) pCMV-Insig-1-T7 or a mutant (m) version (K156R/K158R) as indicated. The total DNA in each lane was adjusted to 3μg/dish by addition of pcDNA3 mock vector. After 16 hr, each dish received 10 μM MG-132. Following incubation at 37 °C for 2 hr, cells were harvested and subjected to immunoprecipitation, SDS-PAGE, and immunoblot analysis as above. Filters were exposed to film for 2-20s.

C) On day 0, SRD-14/pTK-Insig-1-Myc cells (lanes 1-10) and SRD-14/pTK-Insig-1 (K156R/K158R)-Myc cells (lane 11-20) were set up at 5×10^5 cells per 100 mm dish in medium A supplemented with 5% LPDS. On day 2, cells were refed with sterol-depleting medium B. After 16 hr, cells were switched to fresh medium B containing 50 μM CHX in the absence (-) or presence (+) of 1 μg/ml of 25-HC. At the indicated time after CHX treatment, cells were harvested and fractionated, and aliquots of whole-cell lysates were subjected to 10% SDS-PAGE and immunoblot analysis with 2 μg/ml of monoclonal anti-Myc IgG (against Insig-1). Filters were exposed to film for 30s (lanes 1-10) and 2s (lanes 11-20).

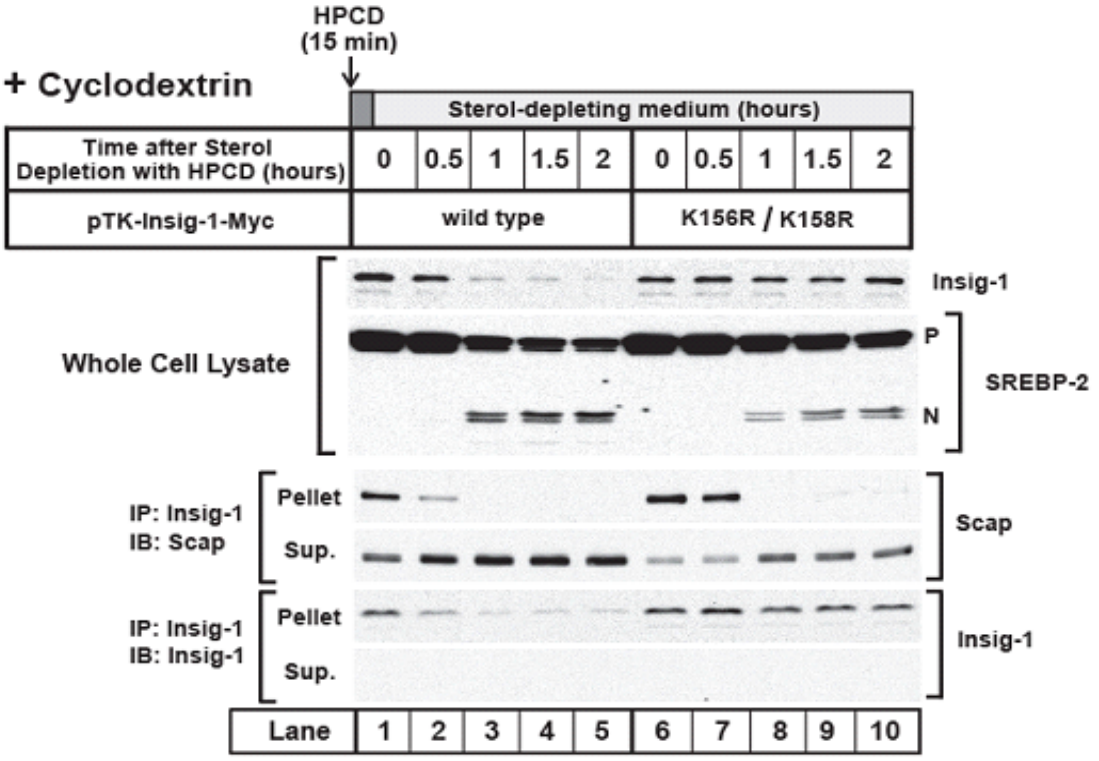
HPCD
(15 min)
+ Cyclodextrin
Sterol-depleting medium (hours)
Time after Sterol Depletion with HPCD (hours)
0 0.5 1 1.5 2 0 0.5 1 1.5 2
pTK-Insig-1-Myc
wild type
K156R / K158R
Whole Cell Lysate
Insig-1
P
N
SREBP-2
IP: Insig-1
IB: Scap
Pellet
Sup.
Scap
IP: Insig-1
IB: Insig-1
Pellet
Sup.
Insig-1
Lane 1 2 3 4 5 6 7 8 9 10

Figure 3-7

Figure 3-7 Time course of SREBP cleavage in Insig-1-deficient hamster cells stably transfected with wild-type or mutant Insig-1 at different times after acute sterol depletion with cyclodextrin.

On day 0, SRD-14/pTK-Insig-1-Myc cells (lanes 1-5) and SRD-14/pTK-Insig-1 (K156R/K158R)-Myc cells (lanes 6-10) were set up at 7×10^5 cells per 60 mm dish in medium A supplemented with 5% LPDS. On day 1, cells were refed with medium A containing 5% LPDS and 0.3 μg/ml of 25-HC. After incubation for 16 hr with 25-HC, the medium was removed and the cells were treated with 1% (w/v) hydroxypropyl-β-cyclodextrin (HPCD) in sterol-free medium B for 15 min, then washed and switched to sterol-free medium B for the indicated time. The switch in medium was staggered such that all the cells could be harvested at the same time and divided into two groups. One group of cells was fractionated, and aliquots of whole-cell lysates were subjected to 8% or 10% SDS-PAGE and immunoblot analysis with 1 μg/ml of monoclonal anti-Myc IgG (against Insig-1) and 5 μg/ml of monoclonal IgG-7D4 (against SREBP-2). P and N denote precursor and nuclear forms of SREBP-2, respectively. The second group of cells was immunoprecipitated (IP) with 40μg/ml polyclonal anti-Myc against Insig-1 as described in Experimental Procedures. Immunoprecipitated pellets (representing 0.25 dish of cells) and supernatants (representing 0.05 dish of cells) were subjected to 8% or 10% SDS-PAGE, and immunoblotted (IB) with 5 μg/ml of monoclonal IgG-9D5 (against Scap) and 1 μg/ml of monoclonal anti-Myc IgG (against Insig-1). Filters were exposed to film for 2-60s.

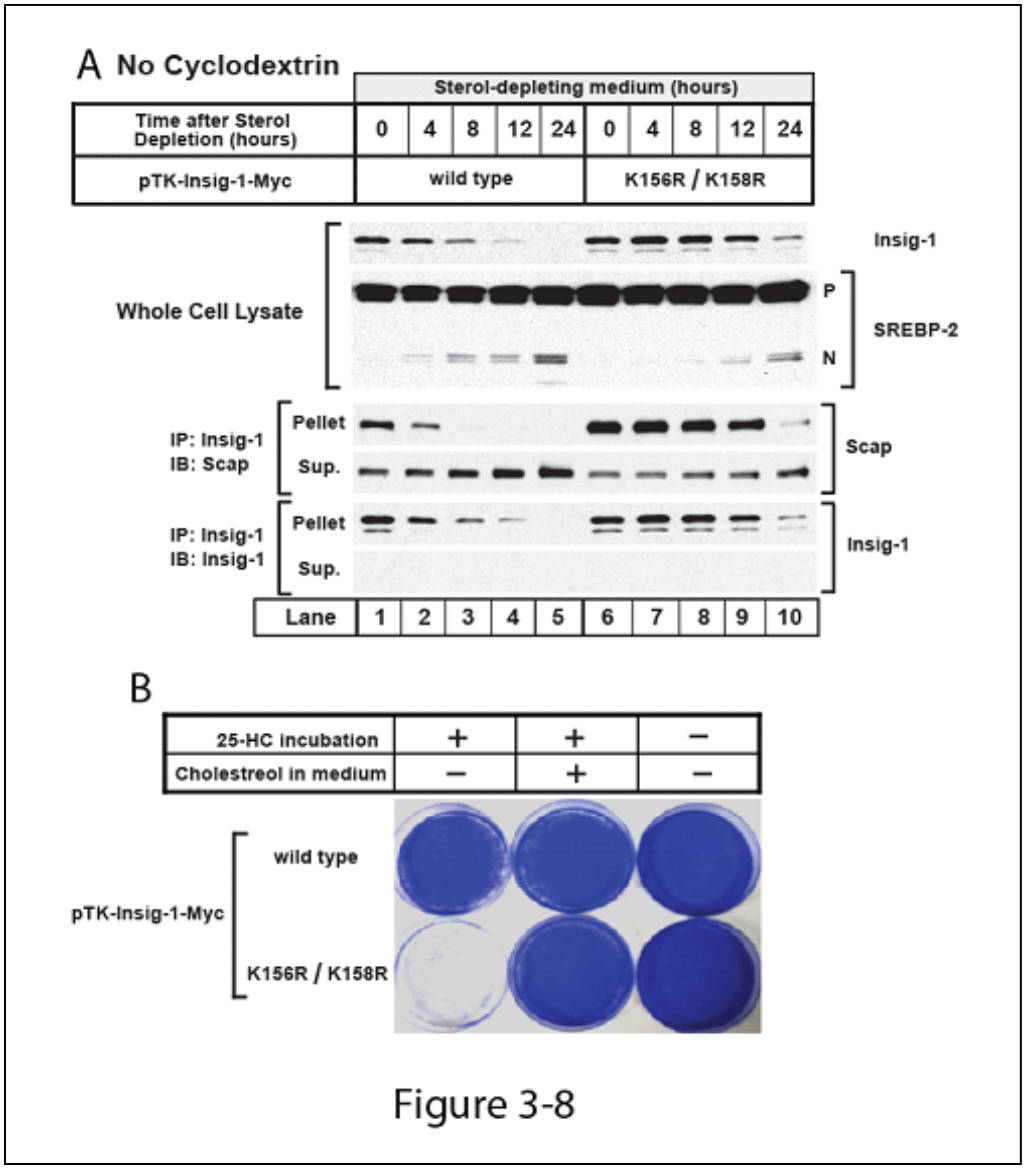
A No Cyclodextrin
Sterol-depleting medium (hours)
Time after Sterol Depletion (hours)
0 4 8 12 24 0 4 8 12 24
pTK-Insig-1-Myc
wild type
K156R / K158R
Whole Cell Lysate
Insig-1
P
N
SREBP-2
IP: Insig-1
IB: Scap
Pellet
Sup.
Scap
IP: Insig-1
IB: Insig-1
Pellet
Sup.
Insig-1
Lane 1 2 3 4 5 6 7 8 9 10
B
25-HC incubation + + −
Cholestreol in medium − + −
pTK-Insig-1-Myc
wild type
K156R / K158R

Figure 3-8

Figure 3-8 Time course of SREBP cleavage in Insig-1-deficient hamster cells stably transfected with wild-type or mutant Insig-1 at different times after gradual sterol depletion.

A) On day 0, SRD-14/pTK-Insig-1-Myc cells (lanes 1-5) and SRD-14/pTK-Insig-1 (K156R/K158R)-Myc cells (lanes 6-10) were set up at 7×10^5 cells per 60 mm dish in medium A supplemented with 5% LPDS. On day 1, cells were refed with medium A containing 5% LPDS and 0.3 μg/ml of 25-HC. After incubation for 12 hr with 25-HC, the cells were washed and then switched to sterol-free medium B for the indicated time. The switch in medium was staggered such that all the cells could be harvested at the same time and divided into two groups. One group of cells was fractionated, and aliquots of whole-cell lysates were subjected to 8% or 10% SDS-PAGE and immunoblot analysis with 1 μg/ml of monoclonal anti-Myc IgG (against Insig-1) and 5 μg/ml of monoclonal IgG-7D4 (against SREBP-2). P and N denote precursor and nuclear forms of SREBP-2, respectively. The second group of cells was immunoprecipitated (IP) with 40μg/ml polyclonal anti-Myc against Insig-1 as described in Experimental Procedures. Immunoprecipitated pellets (representing 0.25 dish of cells) and supernatants (representing 0.05 dish of cells) were subjected to 8% or 10% SDS-PAGE, and immunoblotted (IB) with 5 μg/ml of monoclonal IgG-9D5 (against Scap) and 1 μg/ml of monoclonal anti-Myc IgG (against Insig-1). Filters were exposed to film for 2-60s.

B) On day 0, SRD-14/pTK-Insig-1-Myc cells (lanes 1-5) and SRD-14/pTK-Insig-1 (K156R/K158R)-Myc cells (lanes 6-10) were set up at 1×10^5 cells per 60 mm dish in medium A supplemented with 5% LPDS. On day 1, one group of cells were refed with medium A containing 5% LPDS and 0.3 μg/ml of 25-HC. After incubation for 16 hr with 25-HC, the cells were washed and then switched to sterol-free medium A supplemented with 5% LPDS or sterol-loaded medium C containing 5% (v/v) fetal calf serum, 5 μg/ml cholesterol, 1 mM sodium mevalonate, and 20 μM sodium oleate. Cells were refed every 2 days. On day 14, the cells were washed with PBS, fixed in 95% ethanol, and stained with crystal violet.

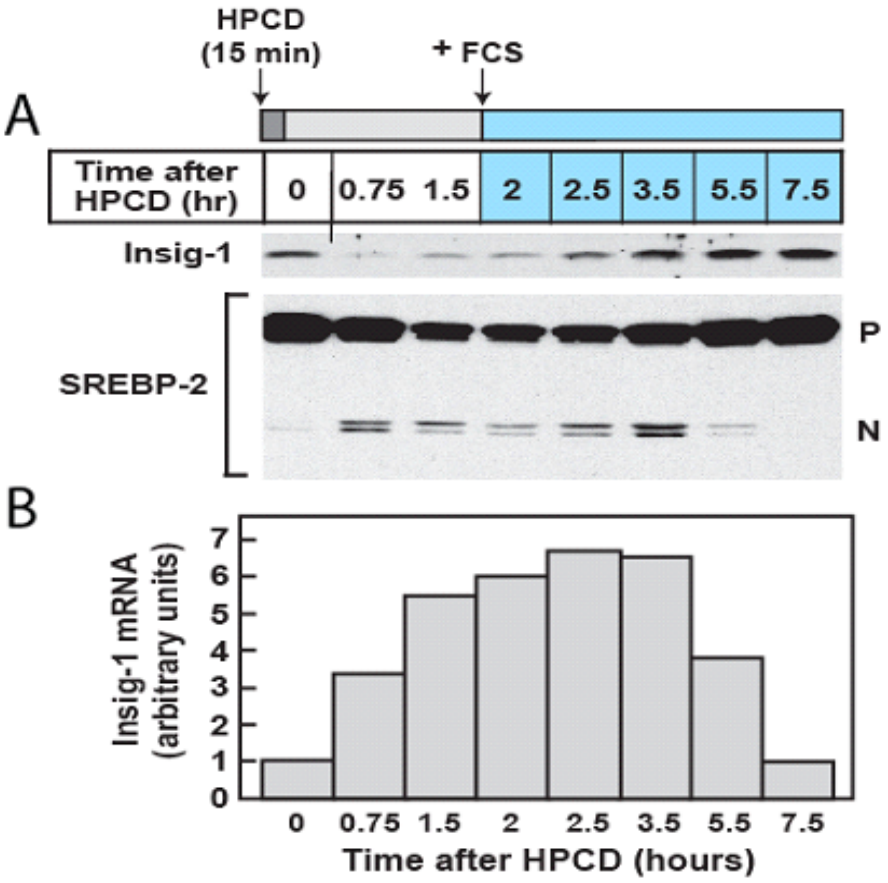
HPCD
(15 min)
+ FCS
A
Time after
HPCD (hr)
0
0.75
1.5
2
2.5
3.5
5.5
7.5
Insig-1
SREBP-2
P
N
B
Insig-1 mRNA
(arbitrary units)
0
1
2
3
4
5
6
7
0
0.75
1.5
2
2.5
3.5
5.5
7.5
Time after HPCD (hours)

Figure 3-9

Figure 3-9 Levels of endogenous Insig-1 protein and mRNA in hamster cells at different times after acute sterol depletion with cyclodextrin followed by incubation with FCS.

On day 0, CHO-7 cells were set up at 5 x 10^5 cells per 100-mm dish in medium A supplemented with 5% LPDS. On day 2, cells were refed with medium A containing 5% LPDS and 0.3 μg/ml of 25-HC. After incubation for 16 hr, the cells were treated with 1% (w/v) hydroxypropyl-β-cyclodextrin (HPCD) in sterol-free medium A supplemented with 5% LPDS for 15 min, then washed and switched to the same sterol-free medium without HPCD for the indicated time. At 1.5 hr after treatment with HPCD, the cells were switched to medium A supplemented with 10% FCS. The switch in medium was staggered such that all the cells could be harvested at the same time and divided into two groups.

A) Cells were harvested and aliquots of whole-cell lysates were subjected to 8% or 10% SDS-PAGE and immunoblot analysis with a 1:1000 dilution of polyclonal antiserum against Insig-1 and 5μg/ml of monoclonal IgG-7D4 (against SREBP-2). P and N denote precursor and nuclear forms of SREBP-2, respectively. Filters were exposed to film for 10s (Insig-1) or 60s (SREBP-2).

B) Cells were harvested and total RNA was isolated from duplicate dishes, pooled, and subjected to reverse transcription as described in Experimental Procedures. Insig-1 mRNA was determined by quantitative real-time PCR. Values are presented in arbitrary units relative to the zero-time value, which is set at 1.

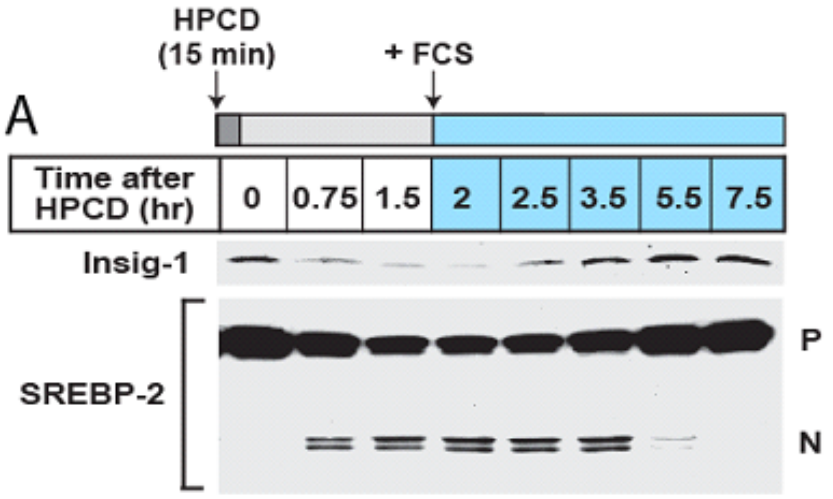
HPCD
(15 min)
+ FCS
A
Time after
HPCD (hr)
0
0.75
1.5
2
2.5
3.5
5.5
7.5
Insig-1
SREBP-2
P
N

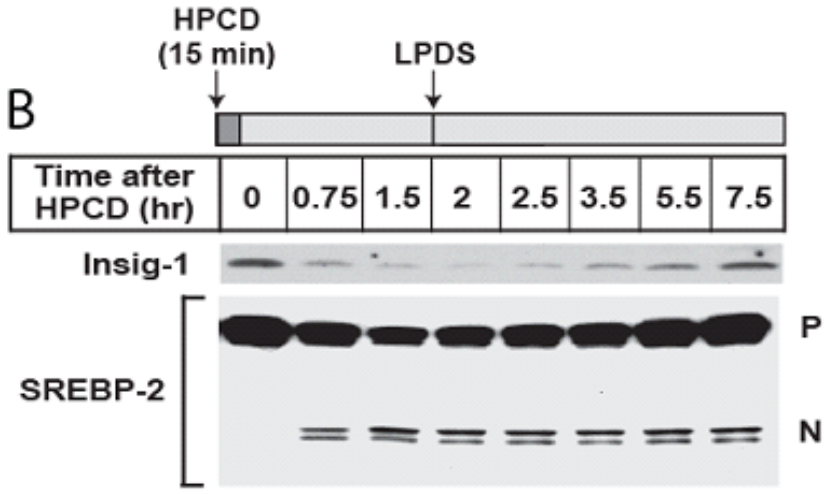
HPCD
(15 min)
LPDS
B
Time after
HPCD (hr)
0
0.75
1.5
2
2.5
3.5
5.5
7.5
Insig-1
SREBP-2
P
N

Figure 3-10

Figure 3-10 Levels of endogenous Insig-1 protein in hamster cells at different times after acute sterol depletion with cyclodextrin followed by incubation with or without FCS.

On day 0, CHO-7 cells were set up at 5 x 10^5 cells per 100-mm dish in medium A supplemented with 5% LPDS. On day 2, cells were refed with medium A containing 5% LPDS and 0.3 μg/ml of 25-HC. After incubation for 16 hr, the cells were treated with 1% (w/v) hydroxypropyl-β-cyclodextrin (HPCD) in sterol-free medium A supplemented with 5% LPDS for 15 min, then washed and switched to the same sterol-free medium without HPCD for the indicated time. At 1.5 hr after treatment with HPCD, the cells were switched to medium A supplemented with either 10% FCS (A) or 5% LPDS (B). The switch in medium was staggered such that all the cells could be harvested at the same time. In (A) and (B), cells were harvested and aliquots of whole-cell lysates were subjected to 8% or 10% SDS-PAGE and immunoblot analysis with a 1:1000 dilution of polyclonal antiserum against Insig-1 and 5μg/ml of monoclonal IgG-7D4 (against SREBP-2). P and N denote precursor and nuclear forms of SREBP-2, respectively. Filters were exposed to film for 10s (Insig-1) or 60s (SREBP-2).

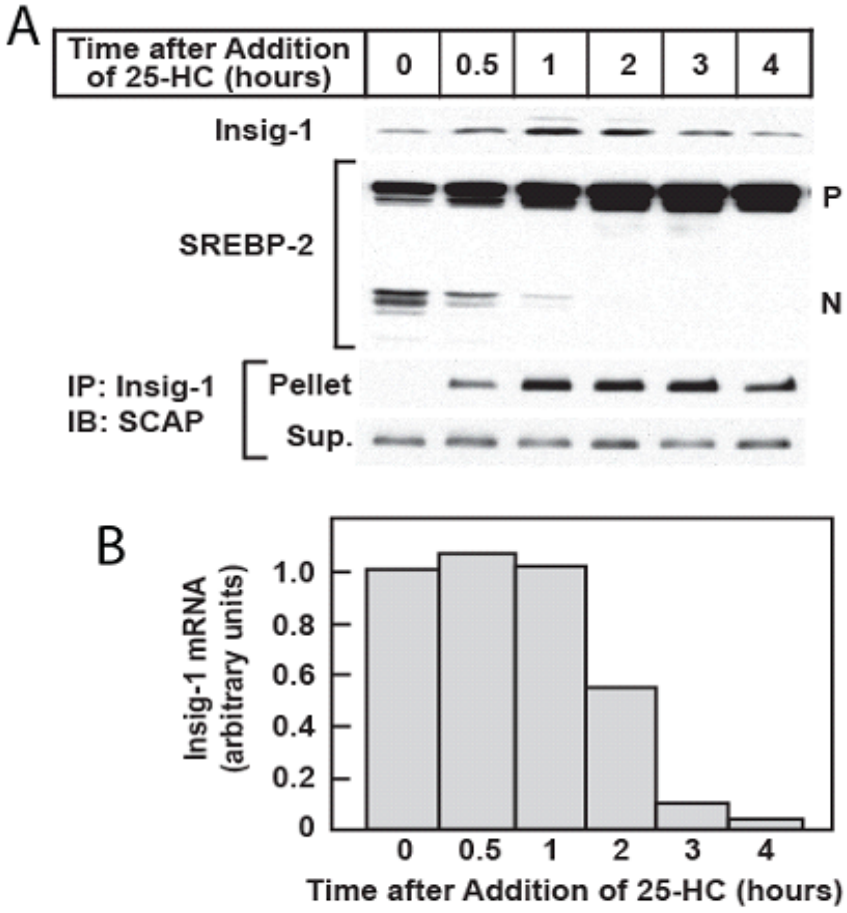
A
Time after Addition of 25-HC (hours)
0
0.5
1
2
3
4
Insig-1
SREBP-2
P
N
IP: Insig-1
IB: SCAP
Pellet
Sup.
B
Insig-1 mRNA (arbitrary units)
1.0
0.8
0.6
0.4
0.2
0
0
0.5
1
2
3
4
Time after Addition of 25-HC (hours)

Figure 3-11

Figure 3-11 Levels of endogenous Insig-1 protein and mRNA in hamster cells at different times after addition of 25-hydroxycholesterol.

On day 0, CHO-7 cells were set up at 5 x 10^5 cells per 100-mm dish in medium A supplemented with 5% LPDS. On day 2, cells were refed with medium B. After 16 hr, cells were switched to medium B containing 1μg/ml of 25-HC. After incubation with 25-HC for the indicated time, the cells were processed for immunoblot analysis (A) and mRNA (B) exactly as described in the legend to Figure 3-9.

Conclusion and future perspective

Sterol-mediated Insig-1/Scap complex formation

The data presented in Chapter 2 provide further evidence that sterol-induced interaction between Scap and Insig-1 is required for feedback inhibition. The direct Insig-1/Scap complex formation is observed through the use of BN-PAGE, and the coimmunoprecipitation experiments further confirmed that this interaction depends strictly on sterols. In addition, a functional role of the Asp-205 in Insig-1 is revealed by site-directed mutagenesis study. Mutations that abolish this negative charge produced an inactive Insig-1 that no longer binds to Scap and fails to ubiquitinate and degrade HMG CoA reductase in the presence of sterols. This brings to one point mutation in Insig-1 that disrupts both Scap/Insig-1 and reductase/Insig-1 complexes in the cells, and results in a sterol-resistant cholesterol synthesis.

Sterol-regulated ubiquitination and degradation of Insig-1

The data presented in Chapter 3 revealed another regulation that sterols impose on Insig-1, namely, the sterol-regulated Insig-1 protein stability. When cells are deprived of sterols, the Insig-1 protein is rapidly ubiquitinated and degraded by proteasomes with a half-life of less than 30 min. When cholesterol is present, cholesterol-loaded Scap binds to Insig-1, thereby stabilizing Insig-1 and preventing its ubiquitination. Thus, in sterol-overloaded cells, Insig-1 has a relatively long half-life (> 2 hr). This stabilization is totally dependent upon Scap. In Scap-deficient cells, cholesterol fails to stabilize Insig-1,

and stability is restored by transfection of a cDNA encoding wild-type Scap, but not the mutant Scap (Y298C) that cannot bind Insigs.

The primary ubiquitination sites of Insig-1 are mapped to lysines at residues 156 and 158. When these two closely spaced lysines are substituted to arginines, Insig-1 ubiquitination is blocked. In consequence, this mutant Insig-1 (K156R/K158R) is not rapidly degraded, and does not require Scap and 25-HC for stabilization. Unlike IκB proteins in NF-κB signaling pathway, ubiquitination and degradation of Insig-1 is not required to release the Scap/SREBP complex when cholesterol is acutely depleted to a low level by cyclodextrin treatment. However, it is important to drive the dissociation of Scap/SREBP from Insig-1 when cholesterol is gradually depleted. Failure to ubiquitinate and degrade Insig-1 causes a marked delay in SREBP processing and cholesterol synthesis in cell growth.

Convergent feedback inhibition of cholesterol synthesis and uptake

The sterol effects on Insig-1 protein stability stand in striking contrast to that on Insig-1 mRNA levels. Inasmuch as Insig-1 is an obligatory SREBP target gene, its mRNA levels are regulated by cholesterol. Thus, when cells are depleted of sterols, Insig-1 mRNA rises owing to cleaved nSREBPs, however, under the same condition Insig-1 protein is rapidly degraded. As a result, Insig-1 transiently decreases to undetectable levels before returning to a steady state (Figures 3-9 and 3-10). When cholesterol accumulates, Insig-1 transcription falls dramatically due to blocked SREBP processing, but Insig-1 protein, instead, is stabilized by sterol-induced binding to Scap. Therefore, Insig-1 transiently increases by 2-3 fold and then drops to a steady state level (Figure 3-11).

The opposite regulation of Insig-1 at two levels (gene transcription and protein stability) leads to a model of "convergent feedback inhibition" for the control of cholesterol supply. The essential elements are diagramed in Figure 4-1. In sterol-depleted cells, cholesterol dissociates from the Scap/SREBP complex, and this causes Insig-1 to dissociate as well. The liberated Insig-1 undergoes ubiquitination at lysines 156 and 158, which leads to proteasomal degradation. The liberated Scap/SREBP complex binds to COPII proteins, which cluster it into COPII-coated vesicles for transport to the Golgi. In the Golgi, the SREBP is processed by proteases to release the transcriptionally active NH2-terminal domain which moves to the nucleus where it activates transcription of all of the genes that encode enzymes required for cholesterol synthesis and for uptake through the LDL receptor. As a result, the cell synthesizes cholesterol and takes it up from LDL to correct the deficit. At the same time, nuclear SREBP enhances transcription of the *Insig-1* gene and the resultant Insig-1 protein is inserted into the ER membrane. The newly synthesized Insig-1 will be degraded rapidly unless the cell has accumulated sufficient cholesterol to alter the conformation of Scap so that it binds Insig-1, forming a stable complex that remains in the ER and resists ubiquitination and degradation. The process is convergent because SREBP processing will not be blocked unless two SREBP products converge on Scap simultaneously: 1) newly synthesized Insig-1, and 2) newly acquired cholesterol. This requirement for convergence assures that SREBP processing will not be terminated prematurely before the SREBP has acted in the nucleus to increase Insig-1 mRNA and to replenish cell cholesterol levels.

Taken together, the studies in this thesis provide compelling evidence that Insig-1 is a master regulator of cholesterol homeostasis through the opposite regulation of Insig-1 protein and the sterol-mediated interaction with Scap.

Future Perspectives

Linking of ubiquitin ligase and Insig-1 degradation

After showing that Insig-1, when freed from Scap, is rapidly ubiquitinated and degraded in proteasomes, and sterol-induced binding of Insig-1 to Scap stabilized Insig-1 by inhibiting its ubiquitination, the questions immediately arise as to which protein is the ubiquitin ligase (E3) responsible for Insig-1 degradation, and what is the mechanism for sterol-dependent inhibition of Insig-1 ubiquitination and degradation.

One potential candidate is a membrane bound E3, gp78, which is identified to associate with Insig-1, and couples sterol regulated ubiquitination and degradation of HMG CoA reductase (Song et al., 2005). In the absence of sterols, Insig-1 binds to the membrane region of gp78. Upon sterols addition, HMG CoA reductase is recruited to this bound Insig-1/gp78 complex, and is subsequently ubiquitinated and degraded. Thus, it is tempting to speculate that in the absence of sterols, when neither Scap nor HMG CoA reductase is bound to Insig-1, gp78 ubiquitinates Insig-1, accelerating its degradation. Since Insig-1 binds constitutively to gp78 in the absence or presence of sterols, the best way to test this hypothesis is to measure the stability of insig-1 after RNAi-mediated knockdown of gp78. If the hypothesis is true, then the ubiquitination and degradation of Insig-1 should be specifically blocked in sterol-depleted cells by siRNA targeting gp78, but not the control siRNA.

Remarkably, when sterols induce reductase to bind to Insig-1, this interaction induces the ubiquitination and degradation of HMG CoA reductase. On the other hand, when sterols induce Scap to bind to Insig-1, it blocks the ubiquitination of Insig-1 and leads to its stabilization. The mechanism by which gp78 fails to ubiquitinate Insig-1 in the presence of sterols is unclear. One possible explanation is that, after forming the Insig-1/Scap complex, the Scap displaces gp78 from Insig-1. Therefore, the gp78 no longer ubiquinates Insig-1. Alternatively, gp78/Insig-1 forms a ternary complex with Scap, yet the lysines 156 and 158 on Insig-1 are not accessible to gp78 any more. The third explanation is that Insig-1/Scap complex might recruit a de-ubiquitin enzyme that removes the polyubiquitin chain from Insig-1. To distinguish all these possibilities, a *in vitro* ubiquitination assay is required to determine the mechanism by which Scap stabilize Insig-1 in a sterol-dependent manner.

Linking of other lipid regulation and Insig-1 protein stability

So far, I have focused on cholesterol mediated Insig-1 protein stability and its role in the feedback regulation of SREBP-2 processing. However, in most cultured cells including the CHO cells used in this study, both SREBP-2 and SREBP-1a are predominant isoforms. As mentioned above, SREBP-2 preferentially activates genes involved in cholesterol biosynthesis and uptake, whereas SREBP-1a is able to activate the entire pathway of cholesterol, fatty acid and triglyceride biosynthesis, as demonstrated in transgenic mice overexpressing transcriptionally active nSREBP-1a in both adipose tissue and liver (Horton et al., 2003). In cultured cells growing in delipidated serum,

addition of polyunsaturated fatty acid such as arachidonic acid could suppress the cleavage of SREBP-1a (Hannah et al., 2001).

Then, does Insig-1 stability also affect SREBP-1 processing? Or, do lipids other than cholesterol affect Insig-1 protein level? The answers to these questions are currently unknown, but worth pursuing. One hint that Insig-1 may also be under the control of fatty acid comes from the recent study of the knockout mice deficient in ELOVL5 gene, which is involved in the of elongation of polyunsaturated fatty acid synthesis. As expected, these mice have no arachidonic acid (20:4) or docosahexaenoic (DHA, 22:6). On a fat fed diet, they overaccumulated cholesterol and triglycerides in liver, and the mRNAs for SREBP target genes in lipogenic pathways were not suppressed (Young-Ah, unpublished results). Interestingly, this phenotype is very similar to what we observed in the Insig-1/-2 double knockout mice, so is there any connection in it? The direct answer to that question is to measure the Insig-1 levels in the mice, and also the Insig-1 protein after polyunsaturated fatty acid treatment in cultured cells.

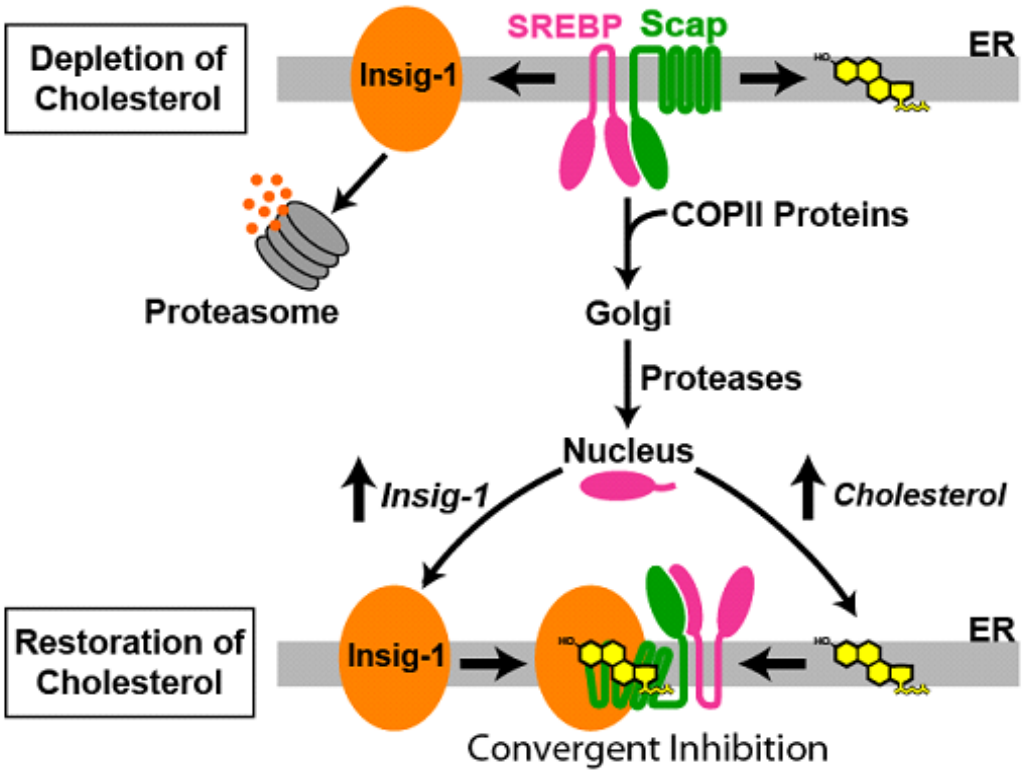
Depletion of Cholesterol
Insig-1
SREBP
Scap
ER
COPII Proteins
Proteasome
Golgi
Proteases
Nucleus
Insig-1
Cholesterol
Restoration of Cholesterol
Insig-1
ER
Convergent Inhibition

Figure 4-1

Figure 4-1 Model for convergent feedback inhibition of cholesterol synthesis and uptake. The essential feature of the model is that SREBP processing will not be blocked by sterols unless two SREBP-induced products converge on Scap simultaneously: (1) newly synthesized Insig-1 and (2) newly synthesized or acquired cholesterol. This convergence assures that SREBP processing will not be terminated before the cholesterol needs of the cell are met.

BIBLIOGRAPHY

Adams, C.M., Goldstein, J.L., and Brown, M.S. (2003). Cholesterol-induced conformational change in SCAP enhanced by Insig proteins and mimicked by cationic amphiphiles. Proc. Natl. Acad. Sci. USA 100, 10647-10652.

Adams, C.M., Reitz, J., DeBrabander, J.K., Feramisco, J.D., Brown, M.S., and Goldstein, J.L. (2004). Cholesterol and 25-hydroxycholesterol inhibit activation of SREBPs by different mechanisms, both involving Scap and insigs. J. Biol. Chem. 279, 52772-52780.

Altmann, S.W., Davis, H.R., Jr., Zhu, L.-J., Yao, X., Hoos, J.M., Tetzloff, G., lyer, S.P.N., Maguire, M., Golovko, A., Zeng, M., et al. (2004). Niemann-Pick C1 like 1 protein is critical for intestinal cholesterol absorption. Science 303, 1201-1204.

Anderson, R.G., Brown, M.S., and Goldstein, J.L. (1977). Role of the coated endocytic vesicles in the uptake of receptor-bound low density lipoprotein in human fibroblasts. Cell 10, 351-364.

Anderson, R.G. Goldstein, J.L., and Brown, M.S. (1976). Localization of low density lipoprotein receptors on plasma membrane of normal human fibroblasts and their absence in cells from a familial hypercholesterolemia homozygote. Proc. Natl. Acad. Sci. USA 73, 2434-2438.

Anderson, R.G. (1998). The caveolae membrane system. Annu. Rev. Biochem. 67, 199-225.

Anderson, R.G. and Jacobson, K. (2002). Cell biology – A role for lipid shells in targeting proteins to caveolae, rafts, and other lipid domains. Science 296, 1821-1825.

Brown, A.J., Sun, L., Feramisco, J.D., Brown, M.S., and Goldstein, J.L. (2002). Cholesterol addition to ER membranes alters conformation of Scap, the SREBP escort protein that regulates cholesterol metabolism. Mol. Cell 10, 237-245.

Brown, M.S., and Goldstein, J.L. (1986). A receptor-mediated pathway for cholesterol homeostasis. Science 232, 34-37.

Brown, M.S., and Goldstein, J.L. (1997). The SREBP pathway: Regulation of cholesterol metabolism by proteolysis of a membrane-bound transcription factor. Cell 89, 331-340.

Brown, M.S., and Goldstein, J.L. (1999). A proteolytic pathway that controls the cholesterol content of membranes, cells, and blood. Proc. Natl. Acad. Sci. USA 96, 11041-11048.

Brown, M.S., Ye, J., Rawson, R.B., and Goldstein, J.L. (2000). Regulated intramembrane proteolysis: A control mechanism conserved from bacteria to humans. Cell 100, 391-398.

Chen, Z.J. (2005). Ubiquitin signaling in the NF-κB pathway. Nat. Cell Biol. 7, 1-8.

Engelking, L.J., Kuriyama, H., Hammer, R.E., Horton, J.D., Brown, M.S., Goldstein, J.L., and Liang, G. (2004). Overexpression of Insig-1 in the livers of transgenic mice inhibits SREBP processing and reduces insulin-stimulated lipogenesis. J. Clin. Invest. 113, 1168-1175.

Engelking, L.J. Liang, G., Hammer, R.E., Takaishi, K., Kuriyama, H., Evers, B.M., Li, W.-P., Horton, J.D., Goldstein, J.L., and Brown, M.S. (2005). Schoenheimer effect explained-feedback regulation of cholesterol synthesis in mice mediated by Insig proteins. J. Clin. Invest. 115, 2489-2498.

Espenshade, P.J., Li, W.-P., and Yabe, D. (2002). Sterols block binding of COPII proteins to SCAP, thereby controlling SCAP sorting in ER. Proc. Natl. Acad. Sci. USA 96, 11694-11699.

Feramisco, J.D., Goldstein, J.L., and Brown, M.S. (2004). Membrane topology of human insig-1, a protein regulator of lipid synthesis. J. Biol. Chem. 279, 8487-8496.

Goldstein, J.L., and Brown, M.S. (1990). Regulation of the mevalonate pathway. Nature 343, 425-430.

Goldstein, J.L., Basu, S.K., and Brown, M.S. (1983). Receptor-mediated endocytosis of low-density lipoprotein in cultured cells. Methods Enzymol. 98, 241-260.

Goldstein, J.L., Rawson, R.B., and Brown, M.S. (2002). Mutant mammalian cells as tools to delineate the sterol regulatory element-binding protein pathway for feedback regulation of lipid synthesis. Arch. Biochem. Biophys. 397, 139-148.

Hannah, V.C., Ou, J., Luong, A., Goldstein, J.L., and Brown, M.S. (2001). Unsaturated fatty acids down-regulate SREBP isoforms 1a and 1c

by two mechanisms in HEK-293 cells. J. Biol. Chem. 276, 4365-4372.

Hershko, A., and Ciechanover, A. (1998). The ubiquitin system. Annu. Rev. Biochem. 67, 425-479.

Hoffmann, A., Levchenko, A., Scott, M.L., and Baltimore, D. (2002). The IκB-NF-κB signaling module: temporal control and selective gene activation. Science 298, 1241-1245.

Horton, J.D., Goldstein, J.L., and Brown, M.S. (2002). SREBPs: activators of the complete program of cholesterol and fatty acid synthesis in the liver. J. Clin. Invest. 109, 1125-1131.

Horton, J.D., Shah, N.A., Warrington, J.A., Anderson, N.N., Park, S.W., Brown, M.S., and Goldstein, J.L. (2003). Combined analysis of oligonucleotide microarray data from transgenic and knockout mice identifies direct SREBP target genes. Proc. Natl. Acad. Sci. USA 100, 12027-12032.

Hua, X., Yokoyama, C., Wu, J., Briggs, M.R., Brown, M.S., Goldstein, J.L., and Wang, X. (1993) SREBP-2, a second basic-helix-loop-helix-leucine zipper protein that stimulates transcription by binding to a sterol regulatory element. Proc. Natl. Acad. Sci. USA 90, 11603-11607.

Hua, X., Nohturfft, A., Goldstein, J.L., and Brown, M.S. (1996). Sterol resistance in CHO cells traced to point mutation in SREBP cleavage-activating protein. Cell 87, 415-426.

Kanayama, A., Seth, R.B., Sun, L., Ea, C.-K., Hong, M., Shaito, A., Chiu, Y.-H., Deng, L., and Chen, Z.J. (2004). TAB2 and TAB3 activate the NF-κB pathway through binding to polyubiquitin chains. Mol. Cell 15, 535-548.

Kita, T., Brown, M.S., and Goldstein, J.L. (1980). Feedback regulation of 3-hydroxy-3-methylglutaryl coenzyme A reductase in livers of mice treated with mevinolin, a competitive inhibitor of the reductase. J. Clin. Invest. 66, 1094-1100.

Kuwabara, P.E., and Labouesse, M. (2002). The sterol-sensing domain: multiple families, a unique role? Trends Genet. 18, 193-201.

Lee, J.N., and Ye, J. (2004). Proteolytic activation of sterol regulatory element-binding protein induced by cellular stress through depletion of Insig-1. J. Biol. Chem. 279, 45257-45265.

Lee, P.C.W., Sever, N., and DeBose-Boyd, R.A. (2005). Isolation of sterol-resistant Chinese hamster ovary cells with genetic deficiencies in both Insig-1 and Insig-2. J. Biol. Chem. 280, 25242-25249.

Luong, A. (2000). Identification of three novel SREBP-activated target genes: acetyl CoA synthetase, 3-β-hydroxysterol dehydrogenase, and CL-6/INSIG1. Ph.D. dissertation. (Dallas: University of Texas Southwestern Medical Center at Dallas) pp. 1-137.

Mann, R.K. and Beachy, P.A. (2004). Novel lipid modifications of secreted protein signals. Annu. Rev. Biochem. 73, 891-923.

Metherall, J.E., Goldstein, J.L., Luskey, K.L., and Brown, M.S. (1989). Loss of transcriptional repression of three sterol-regulated genes in mutant hamster cells. J. Biol. Chem. 264, 15634-15641.

Mosley, S.T., Brown, M.S., Anderson, R.G., and Goldstein, J.L. (1983). Mutant clone of Chinese hamster ovary cells lacking 3-hydroxy-3-methylglutaryl coenzyme A reductase. J. Biol. Chem. 258, 13875-13881.

Nohturfft, A., Brown, M.S., and Goldstein, J.L. (1998). Sterols regulate processing of carbohydrate chains of wild-type SREBP cleavage-activating protein (SCAP), but not sterol-resistant mutants Y298C or D433N. Proc. Natl. Acad. Sci. USA 95, 12848-12853.

Nohturfft, A., Yabe, D., Goldstein, J.L., Brown, M.S., and Espenshade, P.J. (2000). Regulated step in cholesterol feedback localized to budding of SCAP from ER membranes. Cell 102, 315-323.

Radhakrishnan, A., Sun, L.-P., Kwon, H.J., Brown, M.S., and Goldstein, J.L. (2004). Direct binding of cholesterol to the purified membrane region of SCAP: mechanism for a sterol-sensing domain. Mol. Cell 15, 259-268.

Rawson, R.B., DeBose-Boyd, R.A. Goldstein, J.L., and Brown, M.S. (1999). Failure to cleave sterol regulatory element-binding proteins (SREBPs) causes cholesterol auxotrophy in Chinese hamster ovary cells with genetic absence of SREBP cleavage-activating protein. J. Biol. Chem. 274, 28549-28556.

Sakai, J., Duncan, E.A., Rawson, R.B., Hua, X., Brown, M.S., and Goldstein, J.L. (1996). Sterol-regulated release of SREBP-2 from cell membranes requires two sequential cleavages, one within a transmembrane segment. Cell 85, 1037-1046.

Sakai, J., Nohturfft, A., Cheng, D., Ho. Y.K., Brown, M.S., and Goldstein, J.L. (1997). Identification of complexes between the COOH-terminal domains of sterol regulatory element binding proteins (SREBPs) and SREBP cleavage-activating protein (SCAP). J. Biol. Chem. 272, 20213-20221.

Schagger, H., Cramer, W.A., and von Jagow, G. (1994). Analysis of molecular masses and oligomeric states of protein complexes by blue native electrophoresis and isolation of membrane protein complex by two-dimensional native electrophoresis. Anal. Biochem. 217, 220-230.

Sever, N., Song, B.-L., Yabe, D., Goldstein, J.L., Brown, M.S., and DeBose-Boyd, R.A. (2003). Insig-dependent ubiquitination and degradation of mammalian 3-hydroxy-3-methylglutaryl-CoA reductase stimulated by sterols and geranylgeraniol. J. Biol. Chem. 278, 52479-52490.

Sever, N., Lee, P.C.W., Song, B.-L., Rawson, R.B., and DeBose-Boyd, R.A. (2004). Isolation of mutant cells lacking Insig-1 through selection with SR-12813, an agent that stimulates degradation of 3-hydroxy-3-methylglutaryl-CoA reductase. J. Biol. Chem. 279, 43136-43147.

Sever, N., Yang, T., Brown, M.S., Goldstein, J.L., and DeBose-Boyd, R.A. (2003a). Accelerated degradation of HMG CoA reductase mediated by binding of insig-1 to its sterol-sensing domain. Mol. Cell 11, 25-33.

Sever, N., Song, B.-L., Yabe, D., Goldstein, J.L., Brown, M.S., and DeBose-Boyd, R.A. (2003b). Insig-dependent ubiquitination and degradation of mammalian 3-hydroxy-3-methylglutaryl-CoA reductase stimulated by sterols and geranylgeraniol. J. Biol. Chem. 278, 52479-52490.

Simons, K. and Ikonen, E. (1997). Functional rafts in cell membranes. Nature 387, 569-
572.

Simons, K. and Ikonen, E. (2000). How cells handle cholesterol. Science 290, 1721-1726.

Skalnik, D.G., Narita, H., Kent, C., and Simoni, R.D. (1998). The membrane domain of 3-hydroxy-3-methylglutaryl-coenzyme A reductase confers endoplasmic-reticulum localization and sterol-

regulated degradation onto beta-galatosidase. J. Biol. Chem. 263, 6836-6841.

Song, B.-L., Sever, N., and DeBose-Boyd, R.A. (2005). Gp78, a membrane-anchored ubiquitin ligase, associates with Insig-1 and couples sterol-regulated ubiquitination to degradation of HMG CoA reductase. Mol. Cell 19, 829-840.

Sudof, T.C., Russell, D.W., Brown, M.S., and Goldstein, J.L. (1987). 42 bp element from LDL receptor gene confers end-product repression by sterols when inserted into viral TK promoter Cell 48, 1061-1069

Sun, L.-P., Li, L., Goldstein, J.L., and Brown, M.S. (2005). Insig required for sterol-mediated inhibition of Scap/SREBP binding to COPII proteins in vitro. J. Biol. Chem. 280, 26483-26490.

Wang, X., Briggs, M.R., Hua, X., Yokoyama, C., Goldstein, J.L., and Brown, M.S. (1993). Nuclear protein that binds sterol regulatory element of low density lipoprotein receptor promoter. II. Purification and characterization. J. Biol. Chem. 268, 14497-14504.

Yabe, D., Brown, M.S., and Goldstein, J.L. (2002). Insig-2, a second endoplasmic reticulum protein that binds SCAP and blocks export of sterol regulatory element-binding proteins. Proc. Natl. Acad. Sci. USA 99, 12753-12758.

Yabe, D., Xia, Z.-P., Adams, C.M., and Rawson, R.B. (2002). Three mutations in sterol-sensing domain of SCAP block interaction with insig and render SREBP cleavage insensitive to sterols. Proc. Natl. Acad. Sci. USA 99, 16672-16677.

Yabe, D., Komuro, R., Liang, G., Goldstein, J.L., and Brown, M.S. (2003). Liver-specific mRNA for Insig-2 down-regulated by insulin: Implications for fatty acid synthesis. Proc. Natl. Acad. Sci. USA 100, 3155-3160.

Yang, J., Sato, R., Goldstein, J.L., and Brown, M.S. (1994). Sterol-resistant transcription in CHO cells caused by gene rearrangement that truncates SREBP-2. Genes Dev. 8, 1910-1919.

Yang, J., Brown, M.S., Ho, Y.K., and Goldstein, J.L. (1995). Three different rearrangements in a single intron truncate sterol regulatory element binding protein-2 and produce sterol-resistant phenotype in three cell lines. Role of introns in protein evolution. J. Biol. Chem. 270, 12152-12161.

Yang, T., Goldstein, J.L., and Brown, M.S. (2000). Overexpression of membrane domain of SCAP prevents sterols from inhibiting SCAP:SREBP exit from endoplasmic reticulum. J. Biol. Chem. 275, 29881-29886.

Yang, T., Espenshade, P.J., Wright, M.E., Yabe, D., Gong, Y., Aebersold, R., Goldstein, J.L., and Brown, M.S. (2002). Crucial step in cholesterol homeostasis: sterols promote binding of SCAP to INSIG-1, a membrane protein that facilitates of SREBPs in ER. Cell 110, 489-500.

Yokoyama, C., Wang, X., Briggs, M.R., Admon, A., Wu, J., Hua, X., Goldstein, J.L., and Brown, M.S. (1993). SREBP-1, a basic-helix-loop-helix-leucine zipper protein that controls transcription of the low density lipoprotein receptor gene. Cell 75, 187-197.

Zhang, J., Ou, J., Bashmakov, Y., Horton, J.D., Brown, M.S., and Goldstein, J.L. (2001). Insulin inhibitstranscription of IRS-2 gene in rat liver through an insulin response element (IRE) that resembles IREs of other insulin-repressed genes. Proc. Natl. Acad. Sci. USA 98, 37563761.

VITAE

Yi Gong was born in Shanghai, P. R. China on July 9th, 1971, the daughter of Yitai Gong and Liping Fu. She entered Shanghai Medical University in 1989 with a major in medicine. After graduation, she continued her graduate study in the same school and received the master degree in oncology. In 1998, she joined the laboratory of Dr. Tung-Tien Sun in New York University as a visiting scholar. Until 2001, she entered the Graduate School of Biomedical Sciences at the University of Texas Southwestern Medical Center at Dallas where she joined the laboratory of Drs. Brown and Goldstein.

Permanent Address:

542 Qingzhen Road

Shanghai, P. R. China 200233